A new operculate symmoriiform chondrichthyan from the Late Mississippian Fayetteville Shale (Arkansas, United States)

Supplementary Material

Allison W. BRONSON
Department of Biological Sciences, California State Polytechnic University, Humboldt, 1 Harpst Street, Arcata, CA 95521 (United States)
and Division of Paleontology, American Museum of Natural History, Central Park West at 79th Street, New York, NY 10024 (United States)
allison.bronson@humboldt.edu (corresponding author)

Alan PRADEL
Département Origines et Évolution, CR2P UMR 7207 (MNHN, CNRS, Sorbonne Université), Muséum national d'Histoire naturelle, 57 rue Cuvier, 75231 Paris cedex 05 (France)
and Division of Paleontology, American Museum of Natural History, Central Park West at 79th Street, New York, NY 10024 (United States)
alan.pradel@mnhn.fr

John S. S. DENTON
Florida Museum of Natural History, Dickinson Hall, 1659 Museum Road, University of Florida, Gainesville, FL 32611 (United States)
jssdenton@gmail.com

John G. MAISEY
Division of Paleontology, American Museum of Natural History, Central Park West at 79th Street, New York, NY 10024 (United States)
maisey@amnh.org

Bronson A. W., Pradel A., Denton J. S. S. & Maisey J. G. 2024. — A new operculate symmoriiform chondrichthyan from the Late Mississippian Fayetteville Shale (Arkansas, United States). *Geodiversitas* 46 (4): 101-117. https://doi.org/10.5252/geodiversitas2024v46a4. http://geodiversitas.com/46/4

SUPPLEMENTARY FIGURES S1 to S4

SCRIPT FOR PARSIMONY ANALYSIS IN TNT

AIC SCORES FOR LIKELIHOOD ANALYSIS

PARAMETERS FOR LIKELIHOOD ANALYSIS

TAXA INCLUDED IN PHYLOGENETIC ANALYSIS

CHARACTERS USED IN PHYLOGENETIC ANALYSIS

REFERENCES FOR CHARACTER DESCRIPTIONS AND SCORING

SUPPLEMENTARY FIGURES

Supplementary Figure S1. — Photograph of AMNH FF 20509 sent by Royal Mapes to Rainer Zangerl in 1979, showing its pre-pyrite disease condition. Unfortunately, no scale bar was present in the photograph. The specimen is shown in ventral view, anterior to right. However, the distal tip of the right fin (at the top of this image) is actually the counterpart of the tip of the left fin (at the bottom of the image).

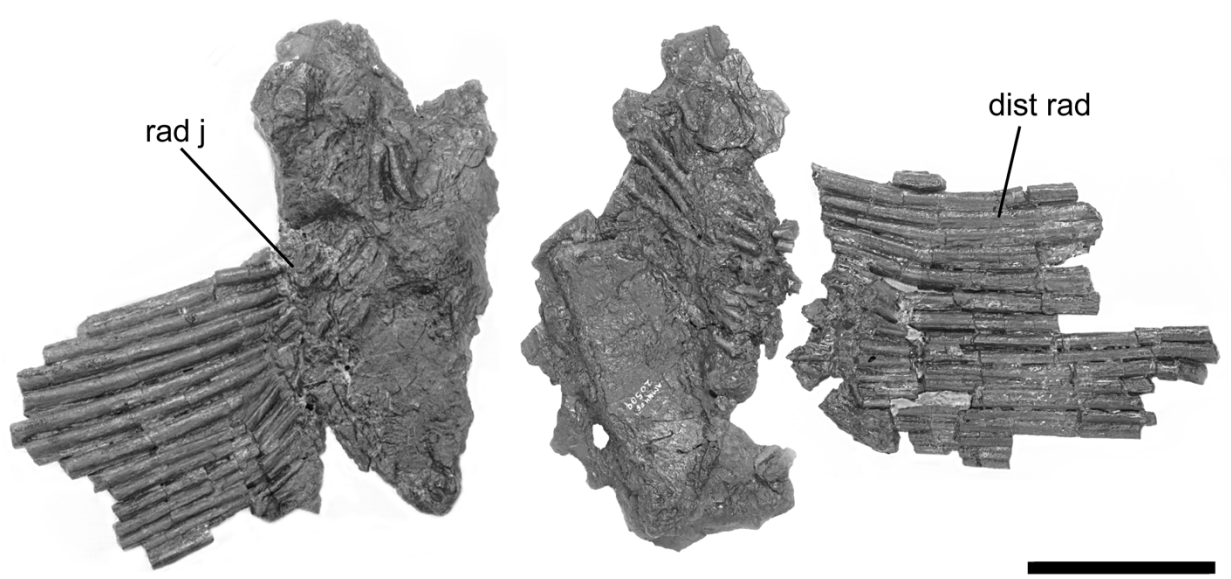

Supplementary Figure S2. — Fins and pectoral cartilages of AMNH FF 20509. Abbreviations: **dist rad**, distal radials; **rad j**, joints between proximal and distal radials. dist rad; Scale bar equals 5 cm.

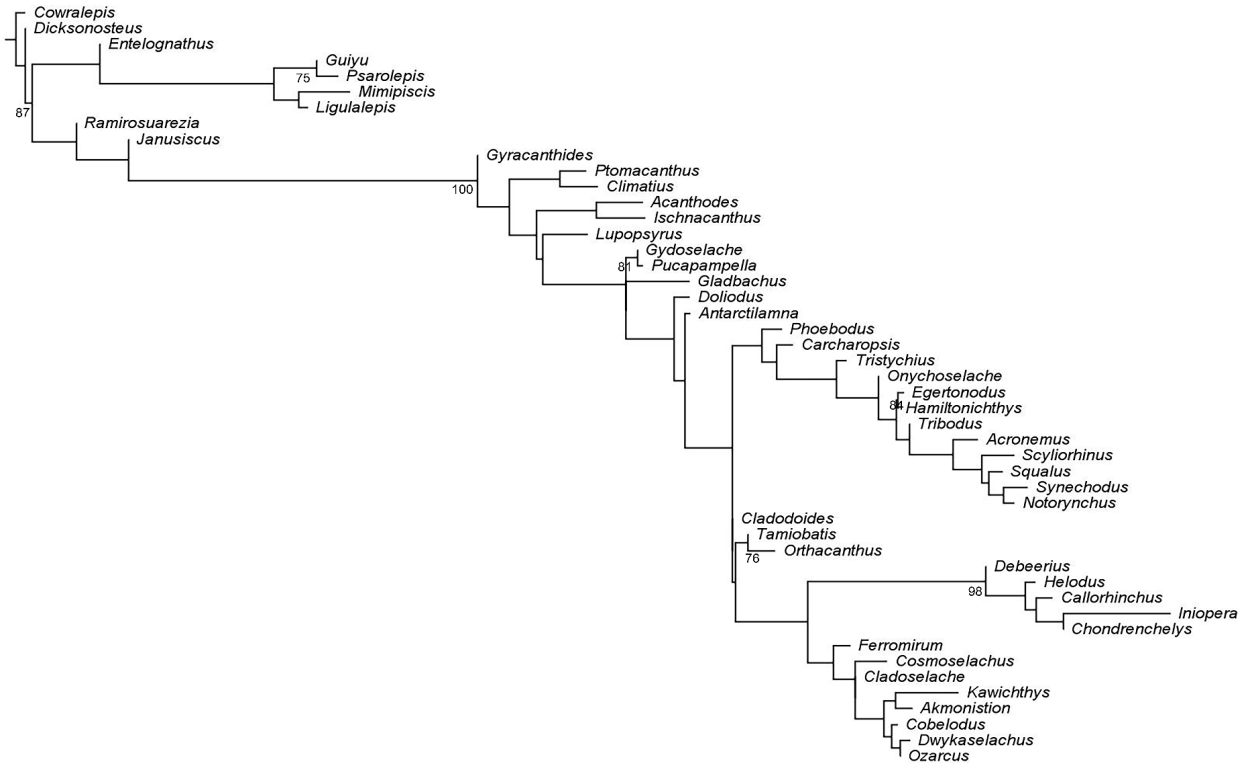

Supplementary Figure S3. — A Lewis / Mkv model was inferred to have the best fit (AIC = 4450.869) to the data when compared with parameterizations under likelihood approximations of parsimony ($AIC_{unweighted}$ = 6018.517; $AIC_{implied}$ = 4759.552) when compared under the Akaike Information Criterion (AIC) in TnT. The four polymorphisms in the matrix were transformed to unknowns (?) to run an Mkv analysis in RAxML, the results of which are shown above (log-likelihood = -2109.6304). The likelihood topology appears resolved due to the nature of parametric phylogenetic analyses, but only bootstrap values above 70 are shown. Interestingly, the tree topology is like the parsimony analysis figured in the main paper, but with the notable difference of a symmoriiform + holocephalan group, sister to other crown chondrichthyans.

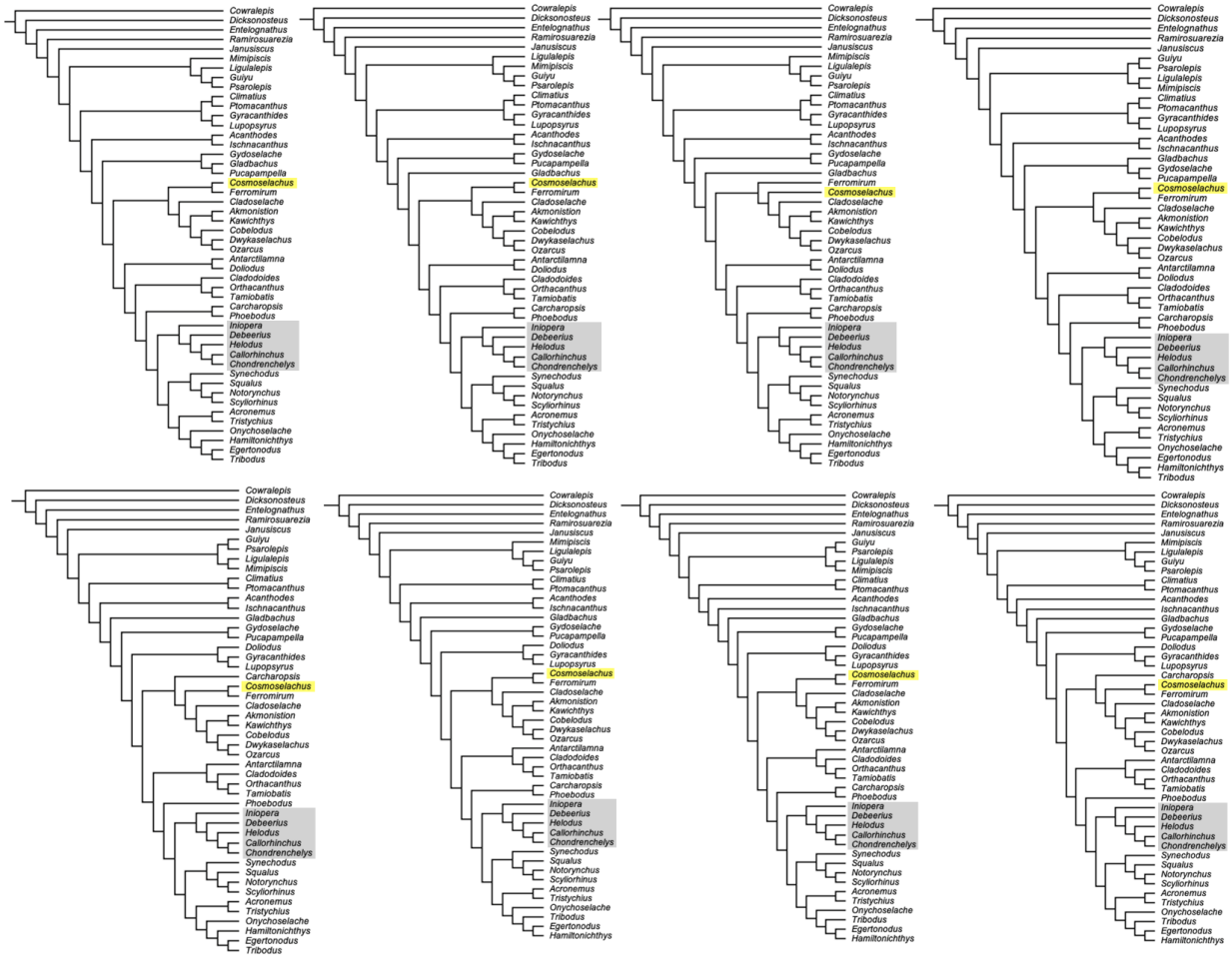

Supplementary Figure S4. — Eight most parsimonious trees generated from the new technology search in TNT, with *Cosmoselachus* highlighted in yellow and the consistent holocephalan clade marked in gray.

SCRIPT FOR PARSIMONY ANALYSIS IN TNT

```
taxname =;

hold 100000;

outgroup Cowralepis;

xmult=hits 10 noupdate nocss replic 10 ratchet 10 fuse 1 drift 5 hold 100 noautoconst keepall;

bbreak = tbr ;

nelsen * ;

export - consensus_tree.tre ;

ttags -;

ttags = ;

resample boot from 1 replic 1000;

keep 1 ;

ttags );

ttags ;

export - ARFossils_ConsensusBoot.tre;

proc/;

comments 0

;
```

AIC SCORES FOR LIKELIHOOD ANALYSIS

model	mk (Lewis Model)	iwa (Implied Weights)	MP (Unweighted Parsimony)	aic-mk	aic-iwa	aic-MP
AIC scores (best-to-worst)	2132.434	2157.776	3008.258	4450.869	4759.552	6018.517

MP better (or equal) to MK = 0

IW better (or equal) to MK = 0

IW better (or equal) to MP = 1

PARAMETERS FOR LIKELIHOOD ANALYSIS

Likelihood analysis with 5 independent ML searches and 1000 bootstraps. Bootstraps mapped onto an optimal tree under the Lewis model + Gamma.

Polymorphisms, e.g. (0 2), transformed to ?

./raxmlHPC-PTHREADS -f a -s ARFossils_Apr30.phy -m ASC_MULTIGAMMA --asc-corr=lewis -# 1000 -x 12345 -p 12345 -n bronson_bootv2

TAXA INCLUDED IN PHYLOGENETIC ANALYSIS

Taxa were scored at the genus level. For oligotypic taxa (*Acanthodes*), we indicated which papers we used for particular species. The genus *Scyliorhinus* includes 16 species, and so we scored for the genus, but individual species' anatomy is described in the cited monograph by Soares & De Carvalho (2019). Taxa in **bold** are absent from Frey et al. 2020.

1. *Acanthodes* Generalized *Acanthodes* characters from (Miles 1968, 1973, 1973; Jarvik 1977, 1980; Coates 1994) Coates 1994; Jarvik 1977; Jarvik 1980; Miles 1968, 1970, 1973a; Nelson 1968; Watson, 1937
    A. lopatini (Beznosov, 2009)
    A. bronni (Brazeau and deWinter, 2015; Davis et al., 2012; Heidtke, 2011a, b)
    A. boyi (Heidtke, 1993)
2. *Acronemus tuberculatus* Maisey, 2011; Rieppel, 1982)
3. *Akmonistion zangerli* (Coates and Sequeira, 1998, 2001a, b; Coates et al., 1998; Coates et al., 2017)
4. ***Antarctilamna prisca*** (Young, 1982)
5. *Callorhinchus milii* (Cole 1896; De Beer 1937; De Beer & Moy-Thomas 1935; Didier 1995; Didier et al. 1994, 1998; Howard et al. 2013; Kesteven 1937; Patterson 1965, 1992; Pradel et al. 2013; Stahl 1999)
6. ***Carcharopsis wortheni*** *(*Bronson et al., 2018; Lund and Mapes, 1984)
7. *Chondrenchelys problematica* (Finarelli and Coates, 2012, 2014; Lund, 1982; Moy-Thomas, 1935)
8. *Cladodoides wildungensis* (Gross, 1937, 1938; Maisey 2005)
9. *Cladoselache* primarily based on *C. fyleri,* but generalized for the genus based on Bendix-Almgreen, 1975; Harris, 1938a, b; Maisey, 1989a, 2007; Schaeffer, 1981; Williams, 2001; Woodward and White, 1938
10. *Climatius* primarily *C. reticulatus*, but generalized for the genus based on Miles, 1973a, b; Watson, 1937
11. *Cobelodus aculeatus* (Zangerl and Case, 1976; Zidek, 1992)
12. ***Cosmoselachus mehlingi*** (this paper)

13. ***Cowralepis mclachlani*** (Ritchie, 2005)
14. *Debeerius ellefseni* (Grogan and Lund, 2000)
15. ***Dicksonosteus arcticus*** (Goujet, 1975)
16. *Doliodus problematicus* (Miller et al., 2003; Maisey et al., 2009, 2014, 2017; Long et al., 2015)
17. *Dwykaselachus oosthuizeni* Coates et al., 2017; Oelofsen, 1986)
18. *Egertonodus basanus* (Maisey, 1982, 1983; Lane, 2010)
19. *Entelognathus primordialis* (Zhu et al., 2013)
20. *Ferromirum oukherbouchi* (Frey et al., 2020)
21. *Gladbachus adentatus* (Heidtke and Krätschmer, 2001; Heidtke, 2009; Burrow and Turner, 2013; Coates et al., 2018)
22. *Guiyu oneiros* (Zhu et al., 2009)
23. *Gydoselache oosthuizeni* (Maisey et al., 2019)
24. *Gyracanthides hawkinsi* (Miles, 1973a; Turner et al., 2005) and *G. murrayi* (Warren et al., 2000)
25. *Hamiltonichthys mapesi* (Maisey, 1989b)
26. *Helodus simplex* (Patterson, 1965; Stahl, 1999)
27. *Iniopera richardsoni* (Zangerl and Case, 1973; Pradel et al., 2009; Pradel, 2010; Pradel et al., 2010)
28. *Ischnacanthus gracilis;* (Miles, 1973a; Watson, 1937)
29. ***Janusiscus schultzei*** **(**Giles et al., 2015a)
30. *Kawichthys moodei* (Pradel et al., 2011)
31. ***Ligulalepis toombsi*** **(**Friedman, 2007; Clement et al., 2018)
32. *Lupopsyrus pygmaeus* (Hanke and Davis, 2012; Bernacsek and Dineley, 1977)
33. *Mimipiscis toombsi* (Gardiner and Bartram, 1977; Gardiner, 1984b; Choo, 2011; Giles and Friedman, 2014)
34. ***Notorynchus cepedianus*** (Wilga, 2002; Maisey 2001, 2004)
35. *Onychoselache traquairi* (Dick and Maisey, 1980; Coates and Gess, 2007)
36. *Orthacanthus* (Hampe, 2002); *O. senckenbergianus* (Heidtke, 1982, 1999); *O. texensis (*Hotton, 1952; Schaeffer, 1981; Maisey, 1983; Lane and Maisey, 2009)
37. *Ozarcus mapesae* (Maisey, 2007; Pradel et al., 2014; Coates et al., 2017)

38. *Phoebodus saidselachus* (Frey et al., 2019)
39. *Psarolepis romeri* (Yu, 1998; Zhu and Schultze, 1997; Zhu et al., 1999; Qu et al., 2013)
40. *Ptomacanthus anglicus* (Brazeau, 2009, 2012; Denison, 1979; Miles, 1973a; Dearden et al., 2019)
41. *Pucapampella rodrigae* (Maisey, 2001c; Maisey and Anderson, 2001; Maisey and Lane, 2010; Janvier and Maisey, 2010; Maisey et al., 2019)
42. ***Ramirosuarezia boliviana*** **(**Pradel et al., 2009b)
43. ***Scyliorhinus*** generalized across 16 species (Soares and De Carvalho, 2019)
44. *Squalus acanthias* (Schaeffer, 1981; Gans and Parsons, 1964; Marinelli and Strenger, 1959)
45. *Synechodus dubrisiensis* (Maisey, 1985)
46. *Tamiobatis vetustus* (Schaeffer, 1981)
47. *Triodus frossardi* (Solér-Gijon and Hampe, 1998; Hampe, 2002; Heidtke et al., 2004)
48. *Tristychius arcuatus* (Dick, 1978; Coates and Gess, 2007; Coates and Tietjen, 2018; Coates et al., 2019)

CHARACTERS USED IN PHYLOGENETIC ANALYSIS

Skeletal Tissues

1. **Intertesseral joint system: absent (0); discontinuous (1); continuous (2)** (Seidel et al., 2016; Coates et al., 2017). An intertesseral joint system is one of the "hallmark" features of conventionally defined chondrichthyans but is more complex than previous investigations have revealed. This system may not be present in some early chondrichthyans (Long et al., 2015), where what was initially described as mineralized matrix between tesserae may instead be endophytic biomineralization (a secondary and possibly pathological condition), as reported in modern elasmobranchs by Seidel et al. (Seidel et al., 2017). The presence of an intertesseral joint system may be variable among pucapampellids, as well as in different parts of the skeleton of a given taxon (Maisey et al., 2020).
2. **Perichondral bone: present (0); absent (1) in adult skeleton.** (Janvier, 1996; Donoghue and Aldridge, 2001; Brazeau, 2009; Davis et al., 2012).
3. **Endochondral ossification throughout endoskeleton: absent (0); present (1).** (Forey, 1980; Gardiner, 1984a; Brazeau, 2009; Davis et al., 2012).
4. **Calcified cartilage throughout endoskeleton: absent (0); present (1).** (Coates et al., 2018)
5. **Dentine histology: mesodentine or semidentine (0); orthodentine (1).** (Donoghue et al., 2000; Brazeau, 2009; Davis et al., 2012). Osteodentine forms the base of all chondrichthyan teeth, but the crown of most teeth is composed primarily of either orthodentine (orthodont teeth, e.g., carcharhiniforms), or osteodentine (osteodont teeth, e.g., lamniforms) (Whitenack et al., 2011). Semidentine is restricted to placoderms, while mesodentine and orthodentine are both found in acanthodians (Chevrinais et al., 2017).
6. **Tubular Dentine: absent (0); present (1).** (Frey et al., 2019).

Dermal Skeleton Including Scales and Fins

7. **Trunk scales monocuspid (0); multicuspid (1).** (Coates et al., 2017). Despite the conclusions of Coates et al. (2017), condition of *Kawichthys* trunk scales is unknown and indicated as such in this analysis.
8. **Scale growth concentric: absent (0); present (1).** (Hanke and Wilson, 2004; Brazeau, 2009; Davis et al., 2012; Burrow et al., 2016).
9. **Body scales with peg and socket type articulation: absent (0); present (1).** (Gardiner, 1984a; Coates, 1999; Brazeau, 2009; Davis et al., 2012). Like the previous character, and *contra* Coates et al. 2017, the state of this character in *Kawichthys* is currently unknown.
10. **Anterodorsal process on scale: absent (0); present (1).** (Gardiner, 1984a; Coates, 1999; Brazeau, 2009; Zhu et al., 2009; Davis et al., 2012; Zhu et al., 2013).
11. **Body scales with bulging (convex) base: absent (0); present (1).** (Brazeau, 2009; Davis et al., 2012).
12. **Body scales with flat base: absent (0); present (1).** (Brazeau, 2009; Davis et al., 2012).
13. **Body scales with basal canal or open basal vascular cavity: absent (0); present (1).** (Coates et al., 2018).
14. **Neck canal: absent (0); present (1).** (Coates et al., 2018)
15. **Flank scale alignment: rhombic packing (0); disorganized (1).** (Davis et al., 2012; Giles et al., 2015a).
16. **Sensory line canal passes between or beneath scales (0); passes over scales and/or is partially enclosed or surrounded by scales (1); perforates and passes through scales (2)**. (Davis, 2002; Friedman and Brazeau, 2010; Davis et al., 2012; Zhu et al., 2013; Brazeau and Friedman, 2014; Burrow et al., 2016).
17. **Lepidotrichia or lepidotrichia-like scale alignment: present (0); absent (1).** (Davis et al. 2012).
18. **Scute-like ridge scales (fulcra): absent (0); present (1).** (Giles et al., 2015b).

Dermal Skeleton of the Skull

19. **Cranial cap denticles, single-crowned, non growing: absent (0); present (1)**. (Frey et al., 2019).
20. **Sclerotic ring: absent (0); present (1).** (Giles *et al*. 2015a, (c.52), Qiao et al., 2016, (c.277), Zhu et al., 2016, (c.275); Burrow et al., 2016; Coates et al., 2018). New observation of *Ozarcus* Synchrotron scans show that it possessed sclerotic rings.
21. **Number of sclerotic plates: four or less (0); more than four (1)**. (Zhu et al., 2013, c170; Qiao et al., 2016, c.241; Zhu et al., 2016, c.239; Burrow et al., 2016).
22. **Dermal skull roof includes large dermal plates (0); consists of undifferentiated plates, scales, or tesserae (1).** (Forey, 1980; Gardiner, 1984a; Brazeau, 2009; Davis et al., 2012; Zhu et al., 2013).
23. **Dermal ornamentation: smooth (0); parallel, vermiform ridges (1); concentric ridges (2); tuberculate (3).** (Giles et al., 2015b).
24. **Enlarged postorbital tessera separate from orbital series**: **absent (0); present (1).** (Brazeau, 2009; Davis et al., 2012; Zhu et al., 2013; Burrow et al., 2016; Frey et al., 2020).
25. **Tessera morphology: large interlocking polygonal plates (0); microsquamose, or not larger than body squamation (1).** (Brazeau, 2009; Davis et al., 2012; Zhu et al., 2013).
26. **Rectilinear skull roof pattern – series of paired median skull roofing bones meeting at the dorsal midline of the skull: absent (0); present (1).** (Brazeau, 2009; Davis et al., 2012; Zhu et al., 2013).
27. **Large, unpaired median bone contributing to the posterior margin of the skull roof: absent (0); present (1).** (Zhu et al., 2013).
28. **Consolidated cheek plates: absent (0); present (1).** (Davis, 2002; Brazeau, 2009; Davis et al., 2012; Zhu et al., 2013).
29. **Parietals (or preorbitals in placoderms) surrounding the pineal foramen or eminence: present (0); absent or uninterrupted suture (1).** (Zhu et al., 2009, 2013).
30. **Dermal intracranial joint: absent (0); present (1).** (Zhu et al., 2009, 2013).

31. **Sensory line network preserved as open sulci or grooves in dermal bones (0); pass through canals enclosed by dermal bones (1).** (Davis et al. 2012; Davis 2002; Zhu et al. 2013).
32. **Sensory canal or pit-line associated with maxilla: absent (0); present (1).** (Coates et al. 2018).
33. **Anterior pit line of skull roof: absent (0); present (1).** (Giles et al., 2015b).

Dermal Skeleton – Operculogular Series

34. **Dermohyal (submarginal) plate: present (0); absent (1).** (Brazeau, 2009; Davis et al., 2012; Zhu et al., 2013).
35. **Branchiostegals (bony hyoidean gill-cover series): absent (0); present (1).** (Davis, 2002; Hanke and Wilson, 2004; Brazeau, 2009; Davis et al., 2012; Zhu et al., 2013; Coates et al., 2017). Following Giles et al. (2015) branchiostegals are coded as present in *Acanthodes*.
36. **Opercular and subopercular bones: absent (0); present (1).** (Coates et al. 2018).
37. **Branchiostegals imbricated: absent (0); present (1).** (Brazeau, 2009; Davis et al., 2012; Zhu et al., 2013).
38. **Opercular cover of branchial chamber complete or partial (0); separate gill covers and gill slits (1).** (Davis et al., 2012).
39. **Endoskeletal operculum: absent (0); present (1).** An opercular flap or cover, supported by endoskeletal branchial arch rays, exists in living holocephalans (living sharks and rays have septate branchial arch rays). *Cosmoselachus* has a similar endoskeletal opercular structure.
40. **Gular plates: absent (0); present (1).** (Gardiner, 1984b; Brazeau, 2009; Davis et al., 2012; Zhu et al., 2013).

Branchial Skeleton

41. **Gill skeleton extends posteriorly beyond occiput: absent (0); present (1).** (Dearden et al., 2019).

42. **First branchial arch meets neurocranium: ventral to otic region (0); posterior to otic region (1).** (Dearden et al. 2019). In *Ozarcus* the suprapharyngobranchial of arch 1 meets the braincase ventral to otic region.
43. **Interhyal: absent (0); present (1).** (Maisey, 1984a; Davis et al., 2012; Zhu et al., 2013).
44. **Ceratohyal posterolateral fossa: absence (0); Presence (1)** (Maisey, 1989a; Coates et al., 2018). This character and the following one are newly created from a character proposed by Coates et al. 2018 (character 69) in order to better depict the different conditions. The posterior, proximal end of some extant elasmobranchs ceratohyals possess a fossa on its lateral surface. The depth of this fossa is varying and appears independent from the lateral bending of the ceratohyal, or the absence/presence of longitudinal groove on the anterolateral surface. This ceratohyal fossa is associated with hyoidean ligaments in *Squalus acanthias* (Haller, 1926; see Maisey 1989 for further information). As discussed in Maisey (1989), this fossa is far from being widespread among extant elasmobranchs, although it occurs sporadically (the best known example being *Odontaspis*; Fürbringer, 1903). In *Scyliorhinus*, the ceratohyal flares laterally posteriorly, but it is not forming a recess or a hollow, whereas the ceratohyal of *Squalus* displays a shallow posterolateral fossa (Marinelli and Strenger, 1959). It is absent in extant holocephalans, as well as some stem forms such as *Iniopera* (new observation suggest that there are posterolateral pits for hyoid rays) (Pradel et al. 2021), *Helodus* and *Debeerius*. Among other fossil chondrichthyans, such a fossa appears to be more widespread than previously suggested. It is present in *Orthacanthus* and *Egertonodus*. In *Gydoselache*, the ceratohyal slightly flares laterally and a small fossa is present posterolaterally (Maisey et al., 2019). Such small fossa looks to be present in the rather straight ceratohyal of *Ozarcus* (Pradel et al., 2014) and *Akmonistion* (Coates and Sequeira, 2001a). Considering the alternative hypothesis that the ‘interhyal’ of *Cladoselache* in Maisey 1989 is actually the internal cast of the ceratohyal posterior lumen, this taxon displays a posterolateral fossa on the ceratohyal. *Gladbachus* also shows a posterolateral ceratohyal recess (Coates et al., 2018).
45. **Longitudinal groove on the lateral surface of the ceratohyals: absent (0); present (1)**. As noted by Coates et al. (2018), the ceratohyals of early osteichthyans, *Acanthodes* and some

Paleozoic chondrichthyans (e.g., *Gladbachus*, *Cladoselache*, *Orthacanthus*, Symmoriiformes) possess a longitudinal groove on the lateral surface of the ceratohyals. It has been suggested that this groove is for the passage of the afferent hyoid artery (Coates et al. 2018). In Modern chondrichthyans, no such groove is present, and the afferent hyoid artery is running ventrally to the ceratohyals (Pradel et al. 2021). This character is independent from the presence of a ceratohyal posterolateral fossa, since they might both accommodate different biological structures which might possess different evolutionary history, some taxa possessing these two features, some only one, some none.

46. **Ceratohyal spatulate or bladed anteriorly: absent (0); present (1).** (Frey et al., 2019).
47. **Hypohyals: absent (0); present (1).** (Friedman and Brazeau, 2010; Pradel et al., 2014; Coates et al., 2017). Following Pradel et al. 2014, *Cladoselache* and *Doliodus* are coded as uncertain. New information suggests that *Iniopera* does not possess hypohyals (Pradel et al. 2021).
48. **Basihyal absent, hyoid arch articulates directly with the basibranchial (0); basihyal present (1).** (Pradel et al., 2014; Coates et al., 2017). Following Pradel et al. (2014), *Cobelodus* is coded as having no basihyal; however, *Orthacanthus* is coded as unknown.
49. **Basibranchial(s) posterior to the basihyal: absent (0); present (1).** This character describes the series of basibranchials posterior to the basihyal, whether there is a single copula such as in many modern elasmobranchs or a continuous series of basibranchials, such as in *Ozarcus* and modern holocephalans.
50. **Perforate hyomandibula: absent (0); present (1).** (Zhu et al., 2009, 2013; Lu et al., 2016; Frey et al., 2020).
51. **Separate supra- and infra-pharyngobranchials absent (0); present (1).** (Gardiner, 1984a; Pradel et al., 2014; Coates et al., 2017).
52. **Pharyngobranchials directed anteriorly (0); posteriorly (1).** (Pradel et al., 2014; Coates et al., 2017).
53. **Posteriormost branchial arch bears epibranchial unit: absent (0); individualized (1); fused to the last pharyngobranchials.** (Coates et al., 2018).

54. **Epibranchials bear posterior flange: absent (0); present (1)**. (Coates et al., 2018). In modern chondrichthyans, the last epibranchial is fused to the last pharyngobranchial. Coded as uncertain in *Akmonistion*.
55. **Multiple unpaired basibranchial mineralizations: absent (0); present (1).** Scored after Frey et al. 2020, particularly with respect to xenacanths and hybodontids. (Dearden et al., 2019; Frey et al., 2020)
56. **Elongate posterior copula projects posteriorly, beyond rearmost branchial arch: absent (0); present (1).** (Frey et al., 2020).
57. **All hypobranchials directed anteriorly (0); hypobranchials of second and more posterior gill arches directed posteriorly (1).** (Maisey, 1984b; Pradel et al., 2014).

Dentition

58. **Oral dermal tubercules borne on jaw cartilages: absent (0); present (1).** (Hanke and Wilson, 2004; Brazeau, 2009; Davis et al., 2012; Zhu et al., 2013). “Rootless teeth,” which rest above a conelike extension of the jaw cartilage, are present in *Pucapampella*, and were likely also present in *Gydoselache* (though none are preserved in the specimen described).
59. **Pharyngeal teeth or denticles: absent (0); present (1).** (Coates et al., 2017). Following Zangerl and Case (1973), *Iniopera* is coded as having pharyngeal denticles (Zangerl and Case, 1973), which are not usually present in crown holocephalans. The distribution of this character among stem holocephalans is unknown.
60. **Tooth families: forming tooth whorls with a continuous basal plate (0); forming tooth whorls, some or all of which consist of separate tooth units (1); absent (2).** (Brazeau, 2009; Davis et al., 2012; Zhu et al., 2013; Maisey et al., 2014). This character reflects whether tooth families form a whorl or not.
61. **Lingual torus: absent (0); present (1).** (Ginter et al., 2010; Coates et al., 2017). The lingual torus is here coded as “absent” in *Pucapampella*, because the “teeth” of this taxon do not have a basal platform (root), but coding as inapplicable would be equally logical. Absence of a lingual torus is considered a euselachian feature.

62. **Basolabial shelf: absent (0); present (1).** (Ginter et al., 2010; Coates et al., 2017).
63. **Tooth whorl restricted to symphysial region (0); distributed along margin of the jaw (1).** (Hanke and Wilson, 2004; Brazeau, 2009; Davis et al., 2012; Zhu et al., 2013).
64. **Toothplates absent (0); present (1).** (Didier, 1995; Coates et al., 2017).
65. **Dermal plates on biting surface of jaw cartilages: absent (0); present (1).** (Brazeau, 2009; Davis et al., 2012; Zhu et al., 2013).
66. **Mandibular teeth fused to dermal plates on biting surfaces of jaw cartilages: absent (0); present (1).** (Hanke and Wilson, 2004; Brazeau, 2009; Davis et al., 2012; Zhu et al., 2013).
67. **Large dermal plates forming outer arcade of biting edge: absent (0); present (1).** (Gardiner, 1984a; Brazeau, 2009; Davis et al., 2012; Zhu et al., 2013).
68. **Parasphenoid: absent (0); present (1).** (Gardiner, 1984a; Brazeau, 2009; Davis et al., 2012; Zhu et al., 2013).
69. **Number of generative tooth sets per jaw ramus: 15 or fewer (0); 20 or more (1).** (Frey et al., 2020).
70. **Teeth with three slim main cusps almost equal to each other, strongly recurved:** absent (0) or present (1). Adapted from Ginter et al. (2010) by Frey et al. (2020).

Mandibular Arch

71. **Large otic process of palatoquadrate: absent (0); present (1).** (Coates and Sequeira, 2001a; Davis, 2002; Brazeau, 2009; Zhu et al., 2009; Davis et al., 2012; Zhu et al., 2013). This was originally described by Coates and Sequeira (2021a) as “Palatoquadrate otic process expanded with an anterodorsal angle,” and by Davis (2002) as simply the presence or absence of an otic process. Here, if the otic process is large enough to be involved in jaw suspension, we have coded this as “present.”
72. **Lateral quadrate expansion above adductor fossa: absent (0); present (1).** A lateral quadrate expansion of the palatoquadrate is present in some hybodontiform chondrichthyans. The dorsal surface of this expansion underlies the postorbital process of the braincase, and the ventral surface forms a roof over the adductor fossa. It is unknown whether this feature is homologous

with the postorbital flange of *Orthacanthus* and *Notorynchus*. Some hybodonts, such as *Acrodus* and *Lissodus* have a sub-postorbital articular groove on the dorsal surface of this lateral quadrate expansion (Thomson, 1982), which is similar to the groove described in *Tristychius* (Dick, 1978).

73. **Oblique ridge or groove along medial face of the palatoquadrate: absent (0); present (1).** (Brazeau, 2009; Davis et al., 2012; Zhu et al., 2013). A groove or ridge is absent in *Pucapampella* and *Gydoselache*.
74. **Perforate or fenestrate anterodorsal (metapterygoid)portion of palatoquadrate: absent (0); present (1)**. (Davis, 2002; Brazeau, 2009; Davis et al., 2012; Zhu et al., 2013).
75. **Articulation surface of the palatoquadrate with the postorbital process directed anteriorly (0); laterally (1); dorsally (2)**. (Coates et al., 2018).
76. **Palatoquadrate fused to the neurocranium: absent (0); present (1).** (Pradel et al., 2011; Coates et al., 2017). *Debeerius* has been scored according to the description in Grogan et al. 2001. *Iniopera* possesses a holostylic condition (Zangerl and Case, 1973; Pradel et al., 2009), and does not have the autodiastylic condition present in other iniopterygians; therefore these two character states are sufficient to describe variation.
77. **Mandibular knob: absent (0); present (1).** (Brazeau, 2009; Davis et al., 2012; Zhu et al., 2013). Coates et al. (2017) scored *Pucapampella* as having no mandibular knob, but it may be present as a weak prominence in *Gydoselache* and in pucapampellid meckelian fragments from Bolivia, so it is here scored as uncertain.
78. **Jaw articulation located on rearmost extremity of the mandible: absent (0); present (1).** (Davis et al., 2012; Zhu et al., 2013).
79. **Dental sulcus (trough) adjacent to oral rim on Meckel's cartilage and palatoquadrate: absent (0); present (1)**. (Coates et al., 2018).
80. **Scalloped oral margin on Meckel's cartilage and palatoquadrate: absent (0); present (1).** (Coates et al., 2017). *Doliodus and Tamiobatis* are coded here as uncertain and *Orthacanthus* is coded as present, *contra* Coates et al. 2017.
81. **Mandibular joint located anteroventral to the rear or the braincase: absent (0); present (1).** The mandibular joint is located anteroventral to the posterior end of the braincase in most crown

chondrichthyans and some Paleozoic chondrichthyans, including *Chondrenchelys, Debeerius, Hamiltonichthys, Helodus, Iniopera, Onychoselache,* and *Tristychius*.

82. **Mandibular symphysis fused: absent (0); present (1).** (Coates et al., 2017).
83. **Dermal plates on mesial (lingual) surfaces of Meckel's cartilage and palatoquadrate: absent (0); present (1).** (Zhu et al., 2013).

Neurocranium

84. **Internasal vacuities: absent (0); present (1)**. (Lu et al., 2016).
85. **Precerebral fontanelle: absent (0); present (1).** (Schaeffer, 1981; Lund and Grogan, 1997; Coates and Sequeira, 1998, 2001a; Maisey, 2001a; Brazeau, 2009; Pradel et al., 2011; Davis et al., 2012; Zhu et al., 2013). In *Kawichthys*, there is a small opening at the front of the braincase (Pradel et al., 2011), which probably represents a small precerebral fontanelle similar to that of other symmoriiform chondrichthyans. *Gydoselache* has an anterior opening homologous to the precerebral fontanelle (Maisey et al., 2019). This feature is unknown in *Pucapampella* because no ethmoid region is preserved. The condition in *Dwykaselachus* is scores as uncertain since a precerebral fontanelle is either absent or reduced (Coates et al. 2017).
86. **Internasal plate separating the two palatoquadrates: absent (0); present (1).** (Pradel et al., 2011). The internasal plate likely separates palatoquadrates of pucapampellids, because they have an ethmoidal articulation.
87. **Space for forebrain and (at least) proximal portion of olfactory tracts narrow and elongate, extending between orbits: absent (0); present (1).** (Coates et al., 2018).
88. **Rostral bar: absent (0); present (1).** (Maisey, 1985).
89. **Internasal groove: absent (0); present (1).** (Coates et al., 2017).
90. **Orbitonasal lamina dorsoventrally deep: absent (0); present (1).** (Patterson, 1965; Davis et al., 2012; Zhu et al., 2013).
91. **Elongate, tooth-bearing, pre-nasal ethmo-rostral region: absent (0); present (1).** (Frey et al., 2020).

92. **Palatobasal or orbital articulation posterior to the optic foramen (0); anterior to optic foramen (1); absent (2).** (Pradel et al., 2011; Coates et al., 2017). Modern chimaeroids and *Debeerius* are coded following interpretations of (Pradel et al., 2011) and (Grogan et al., 1999). *Squalus* is coded as having an orbital articulation posterior to the optic foramen. The orbital articulation of chondrichthyans is here considered homologous to the palatobasal articulation of osteichthyans, based on its similar topographic relationship to the lateral head vein and palatine ramus of the facial nerve (CN VII) (de Beer, 1931) and to the site of the embryonic polar cartilage (Gardiner, 1984b). Some hybodonts may lack this articulation (Dick, 1978), but it may exist in *Acrodus* as the "basal articulation" described by Thomson (Thomson, 1982).
93. **Trochlear foramen anterior to optic nerve: absent (0); present (1).** (Coates and Sequeira, 1998, 2001a; Pradel et al., 2011).
94. **Series of perforations for innervation of the supraorbital sensory canal in supraorbital shelf: absent (0); present (1).** (Giles et al., 2015).
95. **Subcranial ridges: absent (0); present (1).** (Giles et al., 2015).
96. **Supraorbital shelf broad with convex lateral margin: absent (0); present (1).** (Brazeau, 2009; Davis et al., 2012; Zhu et al., 2013).
97. **Optic pedicel: absent (0); present (1).** (Zhu et al., 2009, 2013; Dupret et al., 2014). An attachment area for the optic pedicel is present in pucapampellids.
98. **Ophthalmic foramen in anterodorsal extremity of the orbit communicates with the interior of the cranium: absent (0); present (1).** (Coates et al., 2017).
99. **Canal for efferent pseudobranchial artery within basicranial cartilage: absent (0); present (1).** (Brazeau, 2009; Davis et al., 2012; Zhu et al., 2013).
100. **Bucco-hypophyseal duct open (0); closed (1).** (Coates et al., 2017). Unlike the coding of Coates et al. (2017) *Egertonodus* is coded has having a closed bucco-hypophyseal duct.
101. **Entrance of internal carotids: through separate openings flanking the hypophyseal opening or recess (0); through a common opening at the central midline of the basicranium (1).** (Schaeffer, 1981; Coates and Sequeira, 1998; Brazeau, 2009; Davis et al., 2012; Zhu et al., 2013).

102. **Internal carotids: entering single or paired openings in the basicranium from a posterolateral angle (0); entering basicranial opening(s) head-on from an extreme lateral angle (1); absent (2).** (Coates et al., 2017).
103. **Ascending basisphenoid pillar pierced by the common internal carotid: absent (0); present (1).** (Miles, 1973; Brazeau, 2009; Davis et al., 2012; Zhu et al., 2013). *Iniopera* and chimaeras are coded as absent, because no internal carotid arteries enter the braincase. *Egertonodus* is also scored as absent.
104. **Spiracular groove on basicranial surface: absent (0); present (1).** (Davis et al., 2012; Zhu et al., 2013).
105. **Spiracular groove on lateral or transverse wall of jugular canal: absent (0); present (1).** (Davis et al., 2012; Zhu et al., 2013).
106. **Orbit larger than otic capsule: absent (0); present (1).** (Coates et al., 2017). While this character was resolved as synapomorphy of chimaeroids and symmoriiformes (Coates et al. 2017), examination of Recent elasmobranchs suggests that such features is also present in some modern sharks (e.g., *Scyliorhinus*), hence emphasizing a rather adaptative than phylogenetic pattern of this character.
107. **Chondrified lateral commissure: absent (0); meets the primary postorbital process to form an arcade (1); not connected to the primary postorbital process (2).** (Pradel et al., 2011). Some modern elasmobranchs, such as *Notorynchus*, have only the primary postorbital process present. The lateral commissure of *Squalus* does not reach the primary postorbital process dorsally. In chimaeroids, through there is a postorbital arcade, the latter is not formed by a chondrified lateral commissure (Pradel et al. 2011).
108. **Postorbital articulation: absent (0); on the inferred chondrified lateral commissure (1); on the primary postorbital process (2).** (Pradel et al., 2011).
109. **Postorbital process and arcade short and deep - width not more than maximum braincase width (excluding arcade) (0); process and arcade wide - width exceeds maximum width of braincase, and anteroposteriorly narrow (1); process and arcade massive (2); arcade forms postorbital pillar (3)**. (Coates et al., 2018).

110. **Postorbital process downturned, with anhedral angle relative to basicranium: absent (0); present (1)**. (Maisey, 2011; Coates et al., 2018). The primary process of *Notorynchus* displays an ahedral angle relative to the basicranium (Maisey, 2004).
111. **Jugular vein: passing through a small opening in the chondrified lateral commissure of the postorbital arcade (0); passing through a large opening in the chondrified lateral commissure of the postorbital arcade (1); passing through a cranioquadrate passage (2); not invested into a postorbital canal (3).** (Modified from Pradel et al., 2011 and Coates et al., 2018). See Pradel et al., 2011 for the discussion about the cranioquadrate passage in holocephalans. We consider the state 0 as being present in *Acanthodes*, though the canal is not closed ventrally. The small jugular notch is present through the postorbital arcade formed by a chondrified lateral commissure. As noted by Finarelli & Coates (2014), the condition of *Chondrenchelys* resembles that of some modern holocephalan embryos in having the jugular canal passing through an incomplete cranioquadrate passage (Finarelli and Coates, 2014).
112. **Canal, likely for trigeminal nerve (V) mandibular ramus, passes through the postorbital process from proximal dorsal entry to distal and ventral exit: absent (0); present (1).** (Coates et al., 2018).
113. **Postorbital process expanded anteroposteriorly:** absent (0); present (1). (Coates et al., 2018).
114. **Trigemino-facial recess: absent (0); present (1).** (Goodrich, 1930; Pradel, 2010; Pradel et al., 2011; Davis et al., 2012; Coates et al., 2017). *Akmonistion* is coded as uncertain, and *Doliodus* as present. This feature is absent in *Kawichthys* and uncertain in *Synechodus*.
115. **Jugular canal long, extends throughout most of otic capsule wall posterior to the postorbital process (0); short and/or groove present on exterior of otic wall (1); absent, path of jugular removed from otic wall (2).** (Brazeau, 2009; Davis et al., 2012; Zhu et al., 2013; Giles et al., 2015a; Coates et al., 2017). A jugular groove is present on the lateral wall of the otic region in *Scyliorhinus* (AP personal observation).
116. **C-bout notch, or short canal, separates postorbital process from supraotic shelf: absent (0); present (1).** Modified from Coates et al., (2018). A complete short canal is present between

the dorsal postorbital process and the supraotic shelf in *Scyliorhinus* (AP personal observation). A small notch is present in *Notorynchus* (Maisey, 2004).

117. **Postorbital fossa: absent (0); present (1).** (Zhu et al., 2013).
118. **Hyoid ramus of facial nerve (CN VII) exits through the posterior jugular opening: absent (0); present (1).** (Friedman, 2007; Brazeau, 2009; Friedman and Brazeau, 2010; Davis et al., 2012; Zhu et al., 2013). The hyoid ramus of the facial nerve and the jugular vein share the same foramen in a cranioquadrate passage in *Iniopera* and modern holocephalans (Holmgren, 1942; Pradel, 2010). This cranioquadrate passage was inferred in *Debeerius* (Grogan and Lund, 2000) and *Helodus* (Moy-Thomas, 1936). The condition in *Chondrenchelys* is unknown (Finarelli and Coates, 2014). In *Squalus*, the jugular vein and hyoid ramus exit through separate foramina (Holmgren, 1941).
119. **Posterior postorbital process and supravagal process: absent (0); present (1).** (Coates et al., 2017).
120. **Periotic process: absent (0); present (1).** (Pradel et al., 2011; Coates et al., 2017).
121. **Relative position of jugular groove and hyomandibular articulation: hyomandibula dorsal or same level (i.e. on bridge) (0); jugular vein passing dorsal or lateral to hyomandibula (1)**. (Brazeau and de Winter, 2015).
122. **Transverse otic process: absent (0); present (1).** (Giles et al., 2015a; Lu et al., 2016).
123. **Craniospinal process: absent (0); present (1).** (Giles et al., 2015a; Lu et al., 2016).
124. **Lateral otic process: absent (0); present (1).** (Schaeffer, 1981; Coates and Sequeira, 1998; Brazeau, 2009; Pradel et al., 2011; Davis et al., 2012; Zhu et al., 2013). The presence or absence of this process in *Cladodoides* is unknown (Maisey, 2005).
125. **Hyomandibula articulates with neurocranium beneath otic shelf: absent (0); present (1).** (Coates et al., 2018).
126. **Sub-otic occipital fossa: absent (0); present (1).** (Coates et al., 2017).
127. **Post-otic process: absent (0); present (1).** (Pradel et al., 2011; Coates et al., 2017).
128. **Otic capsule extends posterolaterally relative to occipital arch: absent (0); present (1)**. (Maisey, 1985).

129. **Otic capsules: widely separated (0); approaching dorsal midline (1).** (Coates et al., 2018).
130. **Postorbital arcade: anterior to otic capsule (0); lateral to otic capsule (1).** (Pradel et al., 2011). Contra Coates et al. 2018, the postorbital arcade is lateral to the otic capsule in *Iniopera* (Pradel, 2010), as in modern chimaeroids.
131. **Endocranial roof anterior to otic capsules domelike, smoothly convex dorsally and anteriorly: absent (0); present (1).** (Coates et al., 2018).
132. **Roof of skeletal cavity for cerebellum and mesencephalon significantly higher than the dorsal-most level of the semicircular canals: absent (0); present (1).** (Coates et al., 2017). This feature is likely present in *Kawichthys* (Pradel et al., 2011).
133. **Roof of the endocranial cavity for the telencephalon and olfactory tracts offset ventrally relative to the level of the mesencephalon: absent (0); present (1).** (Coates et al., 2017). Based on the position of the mesencephalon and olfactory tracts, combined with the platybasic condition of the cranium, *Iniopera* is scored as “absent” (Pradel, 2010).
134. **Labyrinth cavity separated from the main neurocranial cavity by an ossified or cartilaginous capsular wall (0); skeletal medial capsular wall absent (1).** (Pradel et al., 2011; Davis et al., 2012; Zhu et al., 2013).
135. **Double octaval nerve foramina in chondrified mesial wall of otic capsule: absent (0); present (1).** (Coates et al., 2018).
136. **Angle of external semicircular canal: in lateral view, straight line projected through canal intersects anterior ampulla, external ampullae, and base of foramen magnum: absent (0); present (1).** (Maisey, 2007; Coates et al., 2018).
137. **Left and right external semicircular canals approach or meet the posterodorsal midine of the hindbrain roof: absent (0); present (1)**. (Coates et al., 2017).
138. **Preampullary portion of posterior semicircular canal absent (0); present (1)**. (Coaetes et al., 2017).
139. **Crus commune connecting anterior and posterior semicircular canals present (0); absent (1).** Modern elasmobranchs exhibit a derived condition in which the posterior semicircular canal is

separated from the anterior canal (Daniel, 1922; Maisey, 1984b, 2001b; Maisey and Lane, 2010; Pradel et al., 2011).

140. **Sinus superior: absent or indistinguishable from union of anterior and posterior canals with saccular chamber (0); present, elongate and nearly vertical (1).** (Davis et al., 2012; Zhu et al., 2013).
141. **Perilymphatic fenestra: absent (0); present (1).** (Pradel et al., 2011; Coates et al., 2017).
142. **Endolymphatic ducts: posteriodorsally angled tubes (0); tubes oriented vertically through median endolymphatic fossa/endolymphatic foramen (1).** (Schaeffer, 1981; Coates and Sequeira, 1998, 2001a; Davis, 2002; Brazeau, 2009; Davis et al., 2012; Zhu et al., 2013).
143. **Posterior dorsal fontanelle extending anterior to crus commune: absent (0); present (1).** This character was modified from Coates et al. (2017, character 105) to accommodate the condition of many Paleozoic sharks, in which the floor of the posterior dorsal fontanelle is non-chondrified, so there is no direct means of establishing the position of the endolymphatic ducts. This is scored as “present” in *Orthacanthus* and *Tamiobatis*.
144. **Posterior dorsal fontanelle connected to persistent otico-occipital fissure (0); posterior tectum separates the fontanelle from the fissure (1).** (Schaeffer, 1981; Coates and Sequeira, 1998; Pradel et al., 2011). The posterior dorsal fontanelle of *Orthacanthus* is ventrally slot-like, and is confluent posteriorly with the otico-occipital fissure (Schaeffer, 1981, p. 22). Contra Coates et al. 2018, the posterior dorsal fontanelle of *Pucapampella* (and *Gydoselache*) is scored as being connected to the persistent otico-occipital fissure Maisey et al. 2019). The character is coded as unapplicable in *Ramirosuarezia* since there is no persistent otico-occipital fissure (Pradel et al., 2009).
145. **Shape of posterior dorsal fontanelle: approximately equal length and breadth (0); far longer than width (1).** (Davis et al., 2012).
146. **Supraotic shelf broad: absent (0); present (1)**. (Coates et al., 2018).
147. **Dorsal otic ridge: absent (0); present (1).** (Coates and Sequeira, 1998, 2001a; Maisey, 2001a; Davis, 2002; Davis et al., 2012; Zhu et al., 2013; Brazeau and Friedman, 2014).

148. **Dorsal otic ridge forms a horizontal crest posteriorly and flanks the anterior rim of the endolymphatic fossa: absent (0); present (1).** (Coates and Sequeira, 1998, 2001a; Pradel et al., 2011).
149. **Endolymphatic or parietal fossa: absent (0); present (1).** (Pradel et al., 2011; Coates et al., 2017). The posterior dorsal fontanelle of *Orthacanthus*, and of many Paleozoic chondrichthyans, is not floored by cartilage. Instead, Schaeffer (1981) notes that "the fossa narrows ventrally, where it joins the endocranial cavity through a slot-like opening, which, in turn, is confluent posteriorly with the otico-occipital fissures," more closely resembling the condition in stem chondrichthyans than that of neoselachians (Schaeffer, 1981). The posterior dorsal fontanelle of *Tamiobatis* is also mainly not floored by cartilage.
150. **Endolymphatic fossa elongate (slot-shaped), dividing dorsal otic ridge along midline: absent (0); present (1)**. (Coates et al., 2017).
151. **Ventral cranial fissure: absent (0); present (1).** (Janvier, 1996; Coates and Sequeira, 2001a; Maisey and Anderson, 2001; Davis, 2002; Brazeau, 2009; Pradel et al., 2011; Davis et al., 2012; Zhu et al., 2013).
152. **Endoskeletal intracranial joint: absent (0); present (1).** (Janvier, 1996; Davis et al., 2012; Zhu et al., 2013).
153. **Metotic (otico-occipital) fissure: absent (0); present (1).** (Schaeffer, 1981; Janvier, 1996; Coates and Sequeira, 1998; Maisey, 2001b; Davis, 2002; Zhu et al., 2013).
154. **Hypotic lamina: absent (0); present (1).** (Schaeffer, 1981; Maisey, 1984, 2001c; Brazeau, 2009; Pradel et al., 2011; Davis et al., 2012; Zhu et al., 2013). Pucapampellids are coded as having a hypotic lamina.
155. **Glossopharyngeal nerve path: crosses the cavity of the auditory capsule and exits anterior to metotic fissure, when present, lateral to the otic capsule (0); exits through the metotic fissure (or remnant of it) posterior to the otic capsule (1).** (Pradel et al., 2011, 2013). Pradel et al. (2013) showed that in extinct holocephalans the glossopharyngeal nerve (CN IX) passes through the remnant of the metotic fissure, as in elasmobranchs. The difference between the condition in elasmobranchs and extinct holocephalans is that neoselachians have a hypotic

lamina, which is absent in chimaeroids. This character specifically refers to the relationship between metotic fissure and glossopharyngeal nerve, while Character 149 deals with the relationship of the glossopharyngeal nerve to the hypotic lamina. Pending ontogenetic data from fossils in which the metotic fissure has closed, the state "1" is inferred if the glossopharyngeal and vagus (CN X) nerve foramina are aligned posterior to the otic capsule (as in chimaeroids and extant neoselachians). Otherwise, the condition is coded as uncertain.

156. **Glossopharyngeal canal floored by the hypotic lamina: absent (0); present (1).** The addition of this character distinguishes between two conditions in taxa that have a hypotic lamina. In modern elasmobranchs, as well as in hybodonts, the hypotic lamina forms the floor of the glossopharyngeal canal, formed by ontogenetic secondary fusion of the lamina and capsular floor. Many Paleozoic chondrichthyans (such as xenacanths, *Cladodoides, Tamiobatis,* and symmoriiforms) have a hypotic lamina, but no fusion has occurred to define a glossopharyngeal canal, and this is also the case in pucapampellids. The condition is unknown in *Doliodus*.
157. **Glossopharyngeal and vagus nerves share common exit from neurocranium: absent (0); present (1)**. (Coates et al., 2018).
158. **Basicranial morphology: platybasic (0); tropibasic (1).** (Brazeau, 2009; Pradel et al., 2011; Davis et al., 2012; Zhu et al., 2013). The condition in *Akmonistion* is unknown (Maisey, 2007).
159. **Interorbital space broad (0); narrow (1).** (Brazeau, 2009; Davis et al., 2012; Zhu et al., 2013; Coates et al., 2017; Frey et al., 2020).
160. **Large prootic foramen separated from optic fenestra by antotic pillar bearing optic pedicel: absent (0); present (1).** Frey et al. (2020), adapted from Maisey et al. (2019).
161. **Extended prehypophysial portion of sphenoid: absent (0); present (1).** (Brazeau, 2009; Davis et al., 2012; Zhu et al., 2013; Frey et al., 2020).
162. **Postorbital process and arcade: absent (0); present (1).** (Pradel et al., 2011; Frey et al., 2020).
163. **Interorbital septum: absent (0); ventral to the endocranial cavity (1); dorsal to the endocranial cavity (2).** (modified from Coates et al., 2017). An interorbital septum is present in some platybasic skulls, such as extant chimaeroids, but is made from the midline fusion of the

orbital cartilages and lies dorsal to the endocranial cavity (de Beer, 1937). In tropibasic crania (such as in modern osteichthyans and probably symmoriiformes), the interorbital septum is formed from a dorsal extension of the trabeculae (de Beer, 1937), so the septum is ventral to the endocranial cavity.

164. **Canal for lateral dorsal aortae within basicranial cartilage: absent (0); present (1).** (Schaeffer, 1981; Coates and Sequeira, 1998; Brazeau, 2009; Pradel, 2010; Pradel et al., 2011; Coates et al., 2018). Contra Coates et al. (2018) and following Pradel (2010), a canal for the lateral dorsal aortae is scored as absent in *Iniopera*.
165. **Medial canal for dorsal aorta within basicranial cartilage: absent (0); present (1).** (Pradel et al., 2011).
166. **Occipital region: overlies paired prebranchial dorsal aortae (0); overlies median prebranchial dorsal aorta (1); overlies postbranchial aortae (2).** This character portrays the three conditions observed in chondrichthyans. In euselachians (elasmobranchs + hybodonts (Maisey, 2012)) and some Paleozoic chondrichthyans, the branchial skeleton is mostly posterior to the occipital region; the prebranchial part of the aortic circuit lies below the braincase. In chimaeroids, the branchial arches are almost wholly subcranial. In both symmoriiformes and modern *Aculeola*, the occipital region overlies an undivided median prebranchial dorsal aorta. In xenacanths, euselachians, *Tamiobatis,* and *Cladodoides*, the occipital region overlies a pair of prebranchial aortae that divided behind the level of the occipital region. The modern holocephalan arrangement is completely different: the occipital region overlies the postbranchial (not prebranchial) part of the aortic circuit. Extinct holocephalans with subcranial branchial arches likely had the same aortic arrangement.
167. **Occipital arch wedged between rear of otic capsules: absent (0); present (1).** (Schaeffer, 1981; Coates and Sequeira, 1998; Maisey, 2001c; Brazeau, 2009; Lane, 2010; Pradel et al., 2011; Davis et al., 2012; Zhu et al., 2013). Symmoriiformes and holocephalans are coded as “present,” in agreement with Pradel et al. (2011)’s interpretation and with Maisey and Lane’s discussion of this character (Maisey and Lane, 2010).

168. **Occipital crest anteroposteriorly elongate, and extends from the roof of the posterior tectum: absent (0); present (1).** (Coates et al., 2017). The condition of *Kawichthys* is uncertain – the rear of the preserved braincase may actually represent the otic-occipital fissure, so it is unknown whether the occipital crest is anteroposteriorly short, terminating at the concave anterior margin of the occipital fissure (as in *Akmonistion, Dwykaselachus,* and *Ozarcus*) or if the crest is formed from the median keel of the posterior tectum and extends posteriorly to the level of the foramen magnum (as in chimaeroids and *Iniopera*).
169. **Subcircular endolymphatic foramen: absent (0); present (1).** (Maisey and Lane, 2010; Janvier and Pradel, 2015; Frey et al., 2020).
170. **External opening for endolymphatic ducts anterior to crus commune: absent (0); present (1).** (Coates et al., 2017; Frey et al., 2020).
171. **Perilymphatic fenestra within the endolymphatic fossa: absent (0); present (1).** (Pradel et al. 2011; Coates et al. 2017).
172. **Unconstricted basicranial notochord: absent (0); present (1).** (Zhu et al., 2009, 2013; Pradel et al., 2011).
173. **Hyomandibular articulation: absent (0); on postorbital process (1); on side wall of otic capsule (2).** (Pradel et al., 2011).
174. **Ectethmoid process: absent (0); present (1).** (Pradel et al., 2011).
175. **Ethmoidal articulation: absent (0); present (1).** (Pradel et al., 2011).
176. **Embryonic basal angle retained in adult: absent (0); present (1).** (Pradel et al., 2011).
177. **Distinct foramina for hyoidean artery: absent (0); present (1).** (Coates and Sequeira, 1998, 2001a; Pradel et al., 2011).
178. **Posterior openings of lateral aortic canals positioned lateral to the occipital cotylus: absent (0); present (1).** (Frey et al. 2020, adapted from Maisey et al. 2019); likely a synapomorphy of pucapampellids. Technically, this character is uninformative in our matrix, as it is present just in *Pucapampella*.

Axial skeleton, paired fins and girdles

179. **Calcified vertebral centra: absent (0); present (1).** (Maisey, 1985; Coates et al., 2017).
180. **Chordacentra: absent (0); present (1).** (Stahl, 1999; Coates and Sequeira, 2001a). Chordacentra (circumchordal rings) are an established feature of holocephalans (Patterson, 1965; Lund, 1982; Finarelli and Coates, 2014); they appear as complete, tightly packed rings in most modern chimaeroids except *Callorhinchus*, and as half-rings that are broader anteroposteriorly in Paleozoic holocephalans (Finarelli and Coates, 2014). Half-ring chordacentra also occur in some symmoriiformes, such as *Damocles* (Lund, 1986). The caudal extremity of *Akmonistion* has a distinctive line that is likely chordacentra, but is here coded as uncertain (Coates and Sequeira, 2001a). No centra are evident in *Debeerius*, so it is coded accordingly (Grogan and Lund, 2000).
181. **Synarcual: absent (0); present (1).** (Stahl, 1999; Brazeau, 2009; Davis et al., 2012; Zhu et al., 2013).
182. **Macromeric dermal pectoral girdle (0); micromeric pectoral girdle or lacking a dermal skeleton entirely (1).** (Brazeau, 2009; Davis et al., 2012; Zhu et al., 2013).
183. **Macromeric dermal pectoral girdle composition: ventral and dorsal components (0); ventral components only (1).** (Brazeau 2009; Davis et al. 2012; Zhu et al. 2013; Frey et al. 2020)
184. **Macromeric pectoral dermal skeleton forms complete ring around the trunk; present (0); absent (1).** (Goujet and Young, 2004; Brazeau, 2009; Davis et al., 2012; Zhu et al., 2013).
185. **Cross sectional shape of scapular process: flattened or strongly ovate (0); subcircular (1).** (Davis, 2002; Brazeau, 2009; Davis et al., 2012; Zhu et al., 2013; Burrow et al., 2016).
186. **Median dorsal plate: absent (0); present (1).** (Brazeau, 2009; Davis et al., 2012; Zhu et al., 2013).
187. **Scapular process (dorsal) of shoulder endoskeleton: absent (0); present (1).** (Coates and Sequeira, 2001a; Zhu and Schultze, 2001; Davis, 2002; Brazeau, 2009; Davis et al., 2012; Zhu et al., 2013; Brazeau and Friedman, 2014).

188. **Scapular process with posterodorsal angle: absent (0); present (1).** (Coates and Sequeira, 2001a; Davis et al., 2012; Zhu et al., 2013). Despite different coding in prior analyses (Giles et al., 2015a; Coates et al., 2017), the condition in *Cladoselache* is unknown.
189. **Mineralisation of internal surface of scapular process: mineralised all around (0); un-mineralised on internal face forming a hemicylindrical cross-section.** (Brazeau, 2009; Davis et al., 2012; Zhu et al., 2013; Burrow et al., 2016).
190. **Scapulocoracoids fused ventrally: absent (0); present (1).** Paired scapulocoracoids are ventrally fused in many living elasmobranchs and in chimaeroids.
191. **Separate procoracoid: absent (0); present (1).** (Giles et al., 2015a).
192. **Fin base articulation on scapulocoracoid: stenobasal, deeper than wide (0); eurybasal, wider than deep (1).** (Lu et al., 2016; Coates et al., 2018).
193. **Number of basals in pectoral fins: three or more (0); two (1); one (2).** (Giles et al., 2015a).
194. **Pectoral fin attachment anterior to metapterygium: individual radial series (0); large basals to which multiple radials are attached (1).** In symmoriiforms, the pectoral fin attaches to the scapulocoracoid by a series of individual radials located anterior to the metapterygium. In xenacanths, crown chondrichthyans, and *Doliodus*, the fins are instead attached by a series of large basals to which multiple radials are attached.
195. **Metapterygial whip: absent (0); present (1).** (Coates and Sequeira, 2001a; Giles et al., 2015a).
196. **Biserial pectoral fin endoskeleton: absent (0); present (1).** (Lu et al., 2016; Coates et al., 2018).
197. **Pelvic girdle with fused pubischiadic bar: absent (0); present (1).** (Maisey, 1984b).
198. **Mixipterygial/misopterygial claspers: absent (0); present (1).** (Maisey, 1984b; Coates and Sequeira, 2001b, 2001a).

Median fins

199. **Number of dorsal fins, if present: one (0); two (1).** (Coates and Sequeira, 2001b; Brazeau, 2009; Davis et al., 2012; Zhu et al., 2013). Contra Coates et al. 2018, *Cladoselache* is scored as having two dorsal fins (Zangerl, 1981).
200. **Posterior or pelvic-level dorsal fin with calcified base plate: absent (0); present (1).** (Coates and Sequeira, 2001a, 2001b). The state in *Tamiobatis* is unknown.
201. **Posterior dorsal fin with delta-shaped cartilage: absent (0); present (1).** (Coates and Sequeira, 2001a, 2001b). Present in many symmoriiforms, such as *Falcatus falcatus* (Lund, 1985) but not present in *Cladoselache*.
202. **Posterior or pelvic-level dorsal fin shape, base approximately as broad as tall and not broader than other median fins (0); base much longer than fin height, substantially longer than other median fins (1).** (Brazeau and Friedman, 2015; Lu et al., 2017).
203. **Anal fin: absent (0); present (1).** (Coates and Sequeira, 2001a, 2001b; Giles et al., 2015). Chimaeroids are scored here as 'present' (Didier 1995).
204. **Caudal radials restricted to axial lobe (0); extend beyond level of body wall and deep into hypochordal lobe (1).** (Davis et al., 2012; Zhu et al., 2013).
205. **Caudal axis upturned steeply, supporting high aspect ratio (lunate) tail: absent (0); present (1).** (Coates and Sequeira, 2001a, 2001b).

Fin spines and other spines of the dermal skeleton

206. **Intermediate (prepelvic) spines: absent (0); present (1).** (Giles et al., 2015a). Recent work shows that *Doliodus* possesses intermediate prepelvic spines like those of some acanthodians (Maisey et al., 2017).
207. **Prepectoral fin spines: absent (0); present (1).** (Giles et al., 2015a). New research shows that *Doliodus* has similar preprectoral spines to those of some acanthodians (Maisey et al., 2017).
208. **Prepectoral fin spines: fused into pineal plate (0); isolated (1).** In many acanthodians (such as *Climatius* and *Ptomacanthus*), the prepectoral fin spines are incorporated into a pineal plate,

but in some acanthodian genera they are represented only by isolated spines. *Doliodus* is coded as having separate prepectoral spines.

209. **Anteriormost intermediate spine associated with shoulder girdle: absent (0); present (1).** (Dearden et al., 2019).
210. **Median fin spine insertion: shallow, not greatly deeper than dermal bones/ scales (0); deep (1).** (Davis, 2002; Hanke and Wilson, 2004; Brazeau, 2009; Davis et al., 2012; Zhu et al., 2013).
211. **Fin spines with ridges: absent (0); present (1).** (Davis, 2002; Brazeau, 2009; Davis et al., 2012; Zhu et al., 2013).
212. **Fin spines with nodes: absent (0); present (1).** (Davis, 2002; Brazeau, 2009; Davis et al., 2012; Zhu et al., 2013).
213. **Fin spines with rows of large retrorse denticles: absent (0); present (1).** (Giles et al., 2015a).
214. **Dorsal fin spines: absent (0); present (1).** (Zhu et al., 2001, 2013; Zhu, 2002; Friedman, 2007; Brazeau, 2009; Davis et al., 2012).
215. **Dorsal fin spines with rows of large denticles on posterior surface: absent (0); present (1).** (Maisey, 1989b; Davis et al., 2012; Zhu et al., 2013).
216. **Dorsal fin spine at anterior (pectoral level) location only: absent (0); present (1).** (Coates and Sequeira, 2001a; Ginter et al., 2010).
217. **Dorsal fin spine cross section: horseshoe shaped (0); flat sided with rectangular profile (1); subcircular (2).** (Hampe and Ivanov, 2007; Brazeau and de Winter, 2015).
218. **Dorsal fin spine apex curved posteriorly: absent (0); present (1).** (Frey et al., 2020), marked present in *Ferromirum* and *Cladoselache*.
219. **Anterior dorsal fin spine leading edge concave in lateral view: absent (0); present (1)**. (Coates et al., 2018).
220. **Anal fin spine: absent (0); present (1).** (Maisey, 1986; Davis, 2002; Brazeau, 2009).
221. **Pectoral fin spines: absent (0); present (1).** (Davis, 2002; Brazeau, 2009; Davis et al., 2012; Zhu et al., 2013).
222. **Cephalic spines: absent (0); present (1).** (Maisey, 1989b).

REFERENCES FOR CHARACTER DESCRIPTIONS AND SCORING

Bernacsek, G. M., and D. L. Dineley. 1977. New acanthodians from the Delorme Formation (Lower Devonian) of N.W.T., Canada. *Paleontographica Abt.A* 158:1–25.

Beznosov, P. 2009. A redescription of the Early Carboniferous acanthodian *Acanthodes lopatini* Rohon, 1899. Acta Zoologica 90(1):183–193.

Brazeau, M. D. 2009. The braincase and jaws of a Devonian "acanthodian" and modern gnathostome origins. Nature 457:305–308.

Brazeau, M. D. 2012. A revision of the anatomy of the early Devonian jawed vertebrate *Ptomacanthus anglicus* Miles. Palaeontology 55:355–367.

Brazeau, M. D., and M. Friedman. 2014. The characters of Palaeozoic jawed vertebrates. Zoological Journal of the Linnean Society 170:779–821.

Brazeau, M. D., and V. de Winter. 2015. The hyoid arch and braincase anatomy of *Acanthodes* support chondrichthyan affinity of 'acanthodians. 'Proceedings of the Royal Society B: Biological Sciences 282:20152210.

Brazeau, M. D., and M. Friedman. 2015. The origin and early phylogenetic history of jawed vertebrates. Nature 520:490–497.

Bronson, A. W., R. Mapes, and J. G. Maisey. 2018. Chondrocranial morphology of *Carcharopsis wortheni* (Chondrichthyes, Euselachii *incertae sedis*) based on new material from the Fayetteville Shale (upper Mississippian, middle Chesterian). Papers in Palaeontology 4(3):349–362.

Burrow, C. J., and S. Turner. 2013. Scale structure of the putative chondrichthyan *Gladbachus adentatus* Heidtke & Krätschmer, 2001 from the Middle Devonian Rheinisches Schiefergebirge, Germany. Historical Biology 25:385–390.

Burrow, C., J. den Blaauwen, M. Newman, and R. Davidson. 2016. The diplacanthid fishes (Acanthodii, Diplacanthiformes, Diplacanthidae) from the Middle Devonian of Scotland. Palaeontologia Electronica 19.1.10A:1–83.

Chevrinais, M., J. Sire, and R. Cloutier. 2017. From body scale ontogeny to species ontogeny: Histological and morphological assessment of the Late Devonian acanthodian *Triazeugacanthus*

affinis from Miguasha, Canada. PLoS ONE 12:e0174655.

Choo, B. 2011. Revision of the actinopterygian genus *Mimipiscis* (=*Mimia*) from the Upper Devonian Gogo Formation of Western Australia and the interrelationships of early Actinopterygii. *Earth and Environmental Science Transactions of the Royal Society of Edinburgh*, 102:77–104.

Clement, A. M., B. King, S. Giles, B. Choo, P. E. Ahlberg, G. C. Young, and J. A. Long. 2018. Neurocranial anatomy of an enigmatic Early Devonian fish sheds light on early osteichthyan evolution. *eLife* **7**:e34349.

Coates, M. I. 1999. Endocranial preservation of a Carboniferous actinopterygian from Lancashire, UK, and the interrelationships of primitive actinopterygians. Philosophical Transactions of the Royal Society B: Biological Sciences 354:435–462.

Coates, M. I., and R. W. Gess. 2007. A new reconstruction of *Onychoselache traquairi*, comments on early chondrichthyan pectoral girdles and hybodontiform phylogeny. Palaeontology, 50(6):1421–1446.

Coates, M. I., and S. E. K. Sequeira. 1998. The braincase of a primitive shark. Transactions of the Royal Society of Edinburgh: Earth Sciences 89:63–85.

Coates, M. I., and S. E. K. Sequeira. 2001a. A new stethacanthid chondrichthyan from the Lower Carboniferous of Bearsden, Scotland. Journal of Vertebrate Paleontology 21:438–459.

Coates, M. I., and S. E. K. Sequeira. 2001b. Early sharks and primitive gnathostome interrelationships; pp. 241–262 in P. E. Ahlberg (ed.), Major Events in Early Vertebrate Evolution. CRC Press.

Coates, M. I. & Tietjen, K. 2018. The neurocranium of the Lower Carboniferous shark *Tristychius arcuatus* (Agassiz, 1837). Earth and Environmental Science Transactions of the Royal Society of Edinburgh 108(1):19–53.

Coates, M. I., I. J. Sansom, and M. M. Smith. 1998. Spines and tissues of ancient sharks. Nature 396:729–730.

Coates, M. I., R. W. Gess, J. A. Finarelli, K. E. Criswell, and K. Tietjen. 2017. A symmoriiform chondrichthyan braincase and the origin of chimaeroid fishes. Nature 541:208–211.

Coates, M. I., J. A. Finarelli, I. J. Sansom, P. S. Andreev, K. E. Criswell, K. Tietjen, M. L. Rivers, and P. J. La Riviere. 2018. An early chondrichthyan and the evolutionary assembly of a shark body plan.

Proc. R. Soc. B 285:20172418.

Coates, M. I., K. Tietjen, A. M. Olsen, and J. A. Finarelli. 2019. High-performance suction feeding in an early elasmobranch. Science Advances 5(9):1–8.

Cole, F. J. 1896. On the cranial nerves of *Chimaera monstrosa* (Linn.); with a discussion of the lateral line system and of the morphology of the chorda tympani. Trans. R. Soc. Edinb. 38: 631–680.

Daniel, J. 1922. The Elasmobranch Fishes. University of California Press, Berkeley, California.

Davis, S. P. 2002. Comparative anatomy and relationships of the acanthodian fishes. University College London.

Davis, S. P., J. A. Finarelli, and M. I. Coates. 2012. *Acanthodes* and shark-like conditions in the last common ancestor of modern gnathostomes. Nature 486:247–250.

Dearden, R. P., C. Stockey, and M. D. Brazeau. 2019. The pharynx of the stem-chondrichthyan *Ptomacanthus* and the early evolution of the gnathostome gill skeleton. Nature Communications 10:1–7.

Denison, R. 1979. Acanthodii. in *Handbook of Paleoichthyology* Vol. 5 (ed. Schultze, H.-P.) Verlag Dr Friedrich Pfeil, 62 pp.

de Beer, G.R. 1937. The Development of the Vertebrate Skull. Oxford Press, Oxford. 554 pp. + 143 pls.

de Beer, G. R. 1931. The development of the skull of *Scyllium (Scyliorhinus) canicula* L. Quarterly Journal of Microscopical Science 74:591–652.

de Beer, G. R. and J. A. Moy-Thomas. 1935. On the skull of Holocephali. Philosophical Transactions of the Royal Society London B 224:287–312.

Dick, J. R. F. 1978. On the Carboniferous shark *Tristychius arcuatus* Agassiz from Scotland. Transactions of the Royal Society of Edinburgh 70:63–109.

Dick, J. R. F. and J. G. Maisey. 1980. The Scottish Lower Carboniferous shark *Onychoselache traquairi*. *Palaeontology* 23:363–374.

Didier, D. A. 1995. Phylogenetic systematics of extant chimaeroid fishes (Holocephali, Chimaeroidei). American Museum Novitates 3119:1–86.

Didier, D. A., B. J. Stahl, and R. Zangerl. 1994. Development and growth of compound tooth plates in *Callorhinchus milii* (Chondrichthyes, Holocephali). Journal of Morphology 222:73–89.

Donoghue, P. C. J., and R. J. Aldridge. 2001. Origin of a mineralized skeleton. In Major Events in Early Vertebrate Evolution (ed. P.E. Ahlberg) pp. 85–105 Systematics Association Special Volume Series 61. Taylor and Francis, London and New York.

Donoghue, P. C. J., P. L. Forey, and R. J. Aldridge. 2000. Conodont affinity and chordate phylogeny. Biological Reviews 75:191–251.

Dupret, V., S. Sanchez, D. Goujet, P. Tafforeau, and P. E. Ahlberg. 2014. A primitive placoderm sheds light on the origin of the jawed vertebrate face. Nature 507:500–503.

Finarelli, J. A., and M. I. Coates. 2012. First tooth-set outside the jaws in a vertebrate. Proceedings of the Royal Society of London Series B-Biological Sciences 279:775–779.

Finarelli, J. A., and M. I. Coates. 2014. *Chondrenchelys problematica* (Traquair, 1888) redescribed: A Lower Carboniferous, eel-like holocephalan from Scotland. Earth and Environmental Science Transactions of the Royal Society of Edinburgh 105:35–59.

Forey, P. L. 1980. *Latimeria*: A paradoxical fish. Proceedings of the Royal Society of London, Series B, Biological Sciences 208:369–384.

Frey, L., M. I. Coates, K. Tietjen, M. Rücklin, and C. Klug. 2020. A symmoriiform from the Late Devonian of Morocco demonstrates a derived jaw function. Communications Biology 3:1–10.

Frey, L., M. Coates, M. Ginter, V. Hairapetian, M. Rücklin, I. Jerjen, and C. Klug. 2019. The early elasmobranch *Phoebodus*: Phylogenetic relationships, ecomorphology and a new time-scale for shark evolution. Proceedings of the Royal Society B: Biological Sciences 286:20191336.

Friedman, M. 2007. *Styloichthys* as the oldest coelacanth: Implications for early osteichthyan interrelationships. Journal of Systematic Palaeontology 5:289–343.

Friedman, M., and M. D. Brazeau. 2010. A reappraisal of the origin and basal radiation of the Osteichthyes. Journal of Vertebrate Paleontology 30:36–56.

Fürbringer, K. 1903. Nachtrag zu meiner abhandlung" Beiträge zur kenntnis des visceralskelets der selachier". Morphol. 31:360–445.

Gans, C. & Parsons, T. S. 1964. *A Photographic Atlas of Shark Anatomy* (Academic Press, New York).

Gardiner, B. G. 1984a. The relationship of placoderms. Journal of Vertebrate Paleontology 4:379–395.

Gardiner, B. G. 1984b. The relationships of the palaeoniscid fishes, a review based on new specimens of

Mimia and *Moythomasia* from the Upper Devonian of Western Australia. Bulletin of the British Museum of Natural History 37:173–428.

Gardiner, B.G. and A.W.H. Bartram. 1977. The homologies of ventral cranial fissures in osteichthyans. In *Problems in Early Vertebrate evolution* S.M. Andrews, R.S. Miles & A.D. Walker, eds. pp. 227-245. Academic Press, London.

Giles, S. and M. Friedman. 2014. Virtual reconstruction of endocast anatomy in early ray-finned fishes (Osteichthyes, Actinopterygii). Journal of Paleontology 88(4):636-651.

Giles, S., M. Friedman, and M. D. Brazeau. 2015a. Osteichthyan-like cranial conditions in an Early Devonian stem gnathostome. Nature 520:82–85.

Giles, S., L. Darras, G. Clément, A. Blieck, and M. Friedman. 2015b. An exceptionally preserved Late Devonian actinopterygian provides a new model for primitive cranial anatomy in ray-finned fishes. Proceedings of the Royal Society B: Biological Sciences 282:20151485.

Ginter, M., O. Hampe, and C. Duffin. 2010. Handbook of Paleoichthyology, Volume 3D: Chondrichthyes - Paleozoic Elasmobranchii: Teeth (H. P. Schultze and O. Kuhn (eds.)). Verlag Dr. Friedrich Pfeil, München, Germany, 168 pp.

Goodrich, E. S. 1930. Studies on the Structure and Development of Vertebrates. Macmillan, London.

Goujet, D., and G. C. Young. 2004. Placoderm anatomy and phylogeny: new insights; pp. 109–126 in G. Arratia, M. V. H. Wilson, and R. Cloutier (eds.), Recent Advances in the Origin and Early Radiation of Vertebrates. Verlag Dr. Friedrich Pfeil, München, Germany.

Grogan, E. D., and R. Lund. 2000. *Debeerius ellefseni* (fam. nov., gen. nov., spec., nov.), an autodiastylic Chondrichthyan from the Mississippian Bear Gulch Limestone of Montana (USA), the relationships of the Chondrichthyes, and comments on gnathostome evolution. Journal of Morphology 243:219–245.

Grogan, E. D., R. Lund, and D. Didier. 1999. Description of the chimaerid jaw and its phylogenetic origins. Journal of Morphology 239:45–59.

Gross, W. 1937. Das Kopfskelett on *Cladodus wildungensis* Jaekel; 1. Teil. Endocranium und Palatoquadratum. Senckenbergiana 19:80–107.

Gross, W. 1938. Das Kopfskelett on *Cladodus wildungensis* Jaekel; 2. Teil. Der Kieferbogen. Anhang:

Protractodus vetusus Jaekel. Senckenbergiana 20:123–145.

Goujet, D., 1975. *Dicksonosteus*, un nouvel arthrodire du Dévonien du Spitsberg remarques sur le squelette visceral des Dolichothoraci. Colloques Internationaux du Centre National de la Recherche Scientifique 218:81–99.

Haller, G. 1926. Uber die entwicklung, den bau und die mechanik des kieferapparates des dornhais (*Acanthias vulgaris*). Z. Mikrosk. Anat. Forsch 749–793.

Hampe, O. 2002. Revision of the Xenacanthida (Chondrichthyes: Elasmobranchii) from the Carboniferous of the British Isles. Trans. R. Soc. Edinb. (Earth Sci.) 93:191–237.

Hampe, O., and A. Ivanov. 2007. Bransonelliformes - A new order of the Xenacanthimorpha (Chondrichthyes, Elasmobranchii). Fossil Record 10:190–194.

Hanke, G. F., and S. P. Davis. 2012. A re-examination of *Lupopsyrus pygmaeus* Bernacsek & Dineley, 1977 (Pisces, Acanthodii). Geodiversitas 34:469–487.

Hanke, G. F., and M. V. H. Wilson. 2004. New teleostome fishes and acanthodian systematics; pp. 189–216 in G. Arratia, M. Wilson, and R. Cloutier (eds.) Recent advances in the origin and early radiation of vertebrates. Verlag Dr Friedrich Pfeil, Munich.

Harris, J. E. 1938a. The dorsal fin spine of *Cladoselache*. Scientific Publications of the Cleveland Museum of Natural History 8:1–6.

Harris, J. E. 1938b. The neurocranium and jaws of *Cladoselache*. Scientific Publications of the Cleveland Museum of Natural History 8:7–12.

Heidtke, U. H. J. 1982. Der Xenacanthide *Orthacanthus senckenbergianus* aus dem pfälzischen Rotliegenden (Unter-Perm). Pollichia 70:65–86.

Heidtke, U. 1993. Studien fiber Acanthodes. 4. *Acanthodes boyi* n.sp., die dritte Art der Acanthodier (Acanthodii: Pisces) aus dem Rotliegend (Unterperm) des Saar-Nahe-Beckens (SW-Deutschland). Paliontologische Zeitschrift 67:331–341.

Heidtke, U. H. J. 1999. *Orthacanthus (Lebachacanthus) senckenbergianus* Fritsch 1889 (Xenacanthida: Chondrichthyes): revision, organisation und phylogenie. Freiberger Forschungsheft 481:63–106.

Heidtke, U. H. J. 2009. *Gladbachus adentatus*, die Geschichte des weltweit ältesten Haisuntersucht und beschriebenaus dem AK Geowissenschaften. *Pollichia Kurrier* **25**, 24-26.

Heidtke, U. H. J. 2011a. Neue Erkenntnisse über *Acanthodes bronni* Agassiz 1833. Mitt. Pollichia 95:1–14.

Heidtke, U. H. J. 2011b. Revision der unterpermischen Acanthodier (Acanthodii: Pisces) des südwestdeutschen Saar-Nahe-Beckens. Mitt. Pollichia 95:15–41.

Heidtke, U. H. J., and K. Krätschmer. 2001. *Gladbachus adentatus* nov. gen. et sp., ein primitiver Hai aus dem Oberen Givetium (Oberes Mitteldevon) der Bergisch Gladbach – Paffrath-Mulde (Rheinisches Schiefergebirge). Mainzer geowiss. Mitt. 30:105–122.

Heidtke, U. H. J., C. Schwind, and K. Krätschmer K. 2004. Über die Organisation des Skelettes und die verwandschaftlichen Beziehungen der Gattung *Triodus* Jordan 1849 (Elasmobranchii: Xenacanthida). Mainzer geowiss. Mitt. 32:9–54.

Holmgren, N. 1941. Studies on the head in fishes part II: Comparative anatomy of the adult selachian skull, with remarks on the dorsal fins in sharks. Acta Zoologica 22:1–100.

Holmgren, N. 1942. Studies on the head in fishes part III: The phylogeny of elasmobranch fishes. Acta Zoologica 23:129–261.

Hotton, N. 1952. Jaws and teeth of American xenacanth sharks. Journal of Paleontology 26:489–500.

Howard, L. E., W. M. Holmes, S. Ferrando, J. S. Maclaine, R. N. Kelsh, A. Ramsey, R. L. Abel, and P. L. J. Cox. 2013. Functional nasal morphology of chimaeroid fishes. Journal of Morphology 274:987–1009.

Janvier, P. 1996. Early Vertebrates. Oxford Science Publications, Bath.

Janvier, P., and J. G. Maisey. 2010. The Devonian vertebrates of South America and their biogeographical relationships. pp. 431–459. In D. K. Elliott, J. G. Maisey, X. Yu, and D. Maio (eds), Morphology, Phylogeny and Paleobiogeography of Fossil Fishes Freidrich Pfeil, Munich.

Janvier, P., and A. Pradel. 2015. Elasmobranchs and their extinct relatives: Diversity, relationships, and adaptations through time. In Physiology of Elasmobranch Fishes: Structure and Interaction with Environment Vol. 34, Part A. (eds. R. E. Shadwock, A. P. Farrel, and C. J. Brauner), pp. 1–17. Elsevier, Inc.

Jarvik, E. 1977 The systematic position of acanthodian fishes. In Problems in vertebrate evolution (eds. SM Andrews, RS Miles, AD Walker), pp. 199–225. Academic Press, London, UK.

Jarvik, E. 1980. Basic structure and evolution of vertebrates, 2 Vols. London: Academic Press.

Kesteven, H. L. 1937. The anatomy of the head of *Callorhynchus antarcticus*. Journal of Anatomy 67:443–474.

Lane, J. a. 2010. Morphology of the braincase in the Cretaceous hybodont shark *Tribodus limae* (Chondrichthyes: Elasmobranchii), based on CT scanning. American Museum Novitates 3681:1–70.

Lane, J. A., and J. G. Maisey. 2009. Pectoral anatomy of *Tribodus limae* (Elasmobranchii: Hybodontiformes) from the Lower Cretaceous of Northeastern Brazil. Journal of Vertebrate Paleontology 29:25–38.

Long, J. A., E. Mark-kurik, Z. Johanson, M. S. Y. Lee, G. C. Young, Z. Min, P. E. Ahlberg, M. Newman, R. Jones, J. den Blaauwen, B. Choo, and K. Trinajstic. 2015. Copulation in antiarch placoderms and the origin of gnathostome internal fertilization. Nature 517:196–199.

Lu, J., S. Giles, M. Friedman, and M. Zhu. 2017. A new stem sarcopterygian illuminates patterns of character evolution in early bony fishes. Nature Communications 8:1932.

Lu, J., S. Giles, M. Friedman, J. L. Den Blaauwen, and M. Zhu. 2016. The oldest actinopterygian highlights the cryptic early history of the hyperdiverse ray-finned fishes. Current Biology 26:1602–1608.

Lund, R. 1982. *Harpagofututor volsellorhinu*s new genus and species (Chondrichthyes, Chondrenchelyiformes) from the Namurian Bear Gulch Limestone, *Chondrenchelys problematica* Traquair (Visean), and their sexual dimorphism. Journal of Paleontology 56:938–958.

Lund, R. 1985. The morphology of *Falcatus falcatus* (St. John and Worthen), a Mississippian stethacanthid chondrichthyan from the Bear Gulch Limestone of Montana. Journal of Vertebrate Paleontology 5:1–19.

Lund, R. 1986. On *Damocles serratus*, nov. gen. et sp. (Elasmobranchii: Cladodontida) from the Upper Mississippian Bear Gulch Limestone of Montana. Journal of Vertebrate Paleontology 6:12–19.

Lund, R., and E. D. Grogan. 1997. Relationships of the Chimaeriformes and the basal radiation of the Chondrichthyes. Reviews in Fish Biology and Fisheries 7:65–123.

Lund, R., and Mapes, R.H., 1984. *Carcharopsis wortheni* from the Fayetteville formation (Mississippian) of Arkansas. Journal of Paleontology 58(3):709–717.

Maisey, J. G. 1982. The anatomy and interrelationships of Mesozoic hybodont sharks. American Museum Novitates 2724:1–48.

Maisey, J. G. 1983. Cranial anatomy of *Hybodus basanus* Egerton from the Lower Cretaceous of England. American Museum Novitates 2758:1–64.

Maisey, J. G. 1984a. Higher elasmobranch phylogeny and biostratigraphy. Zoological Journal of the Linnean Society 82:33–54.

Maisey, J. G. 1984b. Chondrichthyan phylogeny: A look at the evidence. Journal of Vertebrate Paleontology 4:359–371.

Maisey, J. G. 1985. Cranial morphology of the fossil elasmobranch *Synechodus dubrisiensis*. American Museum Novitates 1–28.

Maisey, J. G. 1986. Heads and Tails: a chordate phylogeny. Cladistics 2:201–256.

Maisey, J. G. 1989a. Visceral skeleton and musculature of a Late Devonian shark. Journal of Vertebrate Paleontology 9:174–190.

Maisey, J. G. 1989b. *Hamiltonichthys mapesi*, g. & sp. nov. (Chondrichthyes; Elasmobranchii), from the Upper Pennsylvanian of Kansas. American Museum Novitates 2931:1–42.

Maisey, J. G. 2001a. CT-scan reveals new cranial features in Devonian chondrichthyan *"Cladodus" wildungensis*. Journal of Vertebrate Paleontology 21:807–810.

Maisey, J. G. 2001b. Remarks on the inner ear of elasmobranchs and its interpretation from skeletal labyrinth morphology. Journal of Morphology 264:236–264.

Maisey, J. G. 2001c. A primitive chondrichthyan braincase from the Middle Devonian of Bolivia; pp. 263–288 in P. E. Ahlberg (ed.), Major Events in Early Vertebrate Evolution: Palaeontology, phylogeny, genetics and development. Taylor & Francis Inc., New York.

Maisey, J. G. 2004. Morphology of the braincase in the broadnose sevengill shark *Notorynchus* (Elasmobranchii, Hexanchiformes), based on CT scanning. American Museum Novitates 3429:1–52.

Maisey, J. G. 2005. Braincase of the Upper Devonian Shark *Cladodoides wildungensis* (Chondrichthyes, Elasmobranchii), with observations on the braincase in early chondrichthyans. Bulletin of the American Museum of Natural History 288:1–103.

Maisey, J. G. 2007. The braincase in Paleozoic symmoriiform and cladoselachian sharks. Bulletin of the American Museum of Natural History 307:1–122.

Maisey, J. G. 2011. The braincase of the Middle Triassic shark *Acronemus tuberculatus* (Bassani, 1886). Palaeontology 54:417–428.

Maisey, J. G. 2012. What is an “elasmobranch”? The impact of palaeontology in understanding elasmobranch phylogeny and evolution. Journal of Fish Biology 80:918–951.

Maisey, J. G., and M. E. Anderson. 2001. A primitive chondrichthyan braincase from the Early Devonian of South Africa. Journal of Vertebrate Paleontology 21:702–713.

Maisey, J. G., and J. A. Lane. 2010. Morphologie du labyrinthe et évolution de la phonoréception à basse fréquence chez les élasmobranches. Comptes Rendus - Palevol 9:289–309.

Maisey, J., Miller, R. and Turner, S., 2009. The braincase of the chondrichthyan *Doliodus* from the Lower Devonian Campbellton formation of New Brunswick, Canada. Acta Zoologica, 90:109-122.

Maisey, J. G., S. Turner, G. J. P. Naylor, and R. F. Miller. 2014. Dental patterning in the earliest sharks: Implications for tooth evolution. Journal of Morphology 275:586–596.

Maisey, J. G., J. S. S. Denton, C. Burrow, and A. Pradel. 2020. Architectural and ultrastructural features of tessellated calcified cartilage in modern and extinct chondrichthyan fishes. Journal of Fish Biology98(4)919–941.

Maisey, J. G., R. Miller, A. Pradel, J. S. S. Denton, A. W. Bronson, and P. Janvier. 2017. Pectoral morphology in *Doliodus*: Bridging the ‘acanthodian’- chondrichthyan divide. American Museum Novitates 2017(3875):1–15.

Maisey, J. G., P. Janvier, A. Pradel, J. S. S. Denton, A. W. Bronson, R. Miller, and C. J. Burrow. 2019. *Doliodus* and Pucapampellids: Contrasting perspectives on stem chondrichthyan morphology; pp. 87–109 in Z. Johanson (ed.), Evolution and Development of Fishes.

Marinelli, W., and A. Strenger. 1959. Vergleichen- de Anatomie Und Morphologie Der Wirbelthiere. III. Lieferung, Pt. 2, Squalus Acanthias: Franz Deuticke, Vienna, 179–308 pp.

Miles, R. S., 1968. Jaw articulation and suspension in *Acanthodes* and their significance. Nobel Symposium. Vol. 4. Stockholm: Almqvist and Wiksell.

Miles, R.S., 1970. Remarks on the vertebral column and caudal fin of acanthodian fishes. Lethaia,

3(4):343–362.

Miles, R. S. 1973a. Articulated acanthodian fishes from the Old Red Sandstone of England, with a review of the structure and evolution of the acanthodian shoulder- girdle. Bull. Br. Mus. Nat. Hist. (Geol.) 24:111–213

Miles, R. S. 1973b. Relationships of Acanthodians; pp. in P. H. Greenwood, R. S. Miles, and C. Patterson (eds.), Interrelationships of Fishes. Vol. 53, Supplement no. 1, Zoological Journal of the Linnean Society.

Miller, R.F., R. Cloutier, and S. Turner. 2003. The oldest articulated chondrichthyan from the Early Devonian period. Nature 425(6957):501–504.

Moy-Thomas, J. A. 1935. The structure and affinities of *Chondrenchelys problematica* Tr. Proceedings of the Zoological Society, London 1935:391–403.

Moy-Thomas, J. A. 1936. On the structure and affinities of the Carboniferous cochliodont *Helodus simplex*. Geological Magazine 73:488–503.

Nelson, G.J., 1968. Gill-arches in *Acanthodes*. Current problems of lower vertebrate phylogeny. Almqvist & Wiksell, Stockholm.

Oelofsen, B. W. 1986. A fossil shark neurocranium from the Permo-Carboniferous (lowermost Ecca Formation) of South Africa. In *Indo-Pacific Fish Biology*. Proceedings of the Second International Conference on Indo-Pacific Fishes. Ichthyological Society of Japan, Tokyo, pp. 107–124.

Patterson, C. 1965. The phylogeny of the chimaeroids. Philosophical Transactions of the Royal Society of London. Series B, Biological Sciences 249:101–219.

Patterson, C. 1992. Interpretation of the toothplates of chimaeroid fishes. Zool. J. Linn. Soc. 106:33–61.

Pradel, A. 2010. Skull and brain anatomy of Late Carboniferous Sibyrhynchidae (Chondrichthyes, Iniopterygia) from Kansas and Oklahoma (USA). Geodiversitas 32:595–661.

Pradel, A., M. Langer, J. G. Maisey, D. Geffard-Kuriyama, P. Cloetens, P. Janvier, and P. Tafforeau. 2009a. Skull and brain of a 300 million-year-old chimaeroid fish revealed by synchrotron holotomography. Proceedings of the National Academy of Sciences of the USA 106:5224-5228.

Pradel, A., J. G. Maisey, P. Tafforeau, and P. Janvier. 2009b. An enigmatic gnathostome vertebrate skull from the Middle Devonian of Bolivia. Acta Zoologica 90(Suppl. 1):123-133.

Pradel, A. P. Tafforeau, and P. Janvier. 2010. Study of the pectoral girdle and fins of the Late Carboniferous sybirhynchid iniopteryians (Vertebrata, Chondrichthyes, Iniopterygia) from Kansas and Oklahoma (USA) by means of microtomography, with comments on iniopterygian relationships. Comptes Rendus Palevol 9: 377-387.

Pradel, A., P. Tafforeau, J. G. Maisey, and P. Janvier. 2011. A new paleozoic symmoriiformes (chondrichthyes) from the late carboniferous of Kansas (USA) and cladistic analysis of early chondrichthyans. PLoS ONE 6.

Pradel, A., D. Didier, D. Casane, P. Tafforeau, and J. G. Maisey. 2013. Holocephalan embryo provides new information on the evolution of the glossopharyngeal nerve, metotic fissure and parachordal plate in gnathostomes. PLoS ONE 8:4–9.

Pradel, A., J. G. Maisey, P. Tafforeau, R. H. Mapes, and J. Mallatt. 2014. A Palaeozoic shark with osteichthyan-like branchial arches. Nature 509:608–11.

Pradel A., Dearden R.P., Cuckovic A., Mansuit R. & Janvier P. 2021. — The visceral skeleton and its relation to the head circulatory system of both a fossil, the Carboniferous *Iniopera*, and a modern, *Callorhinchus milii* holocephalan (Chondrichthyes), *in* Pradel A., Denton J.S.S. & Janvier P. (eds.), *Ancient Fishes and their Living Relatives: a Tribute to John G. Maisey*. München, Germany, Verlag Dr. Friedrich Pfeil. p. 183–192.

Qiao, T., B. King, J. A. Long, P. E. Ahlberg, and M. Zhu. 2016. Early gnathostome phylogeny revisited: Multiple method consensus. PLoS ONE 11:e0163157.

Qu, Q., M., Zhu, M. & Wang, W. 2013. Scales and dermal skeletal histology of an early bony fish *Psarolepis romeri* and their bearing on the evolution of rhombic scales and hard tissues. PLoS One 8:e61485.

Rieppel, O. 1982. A new genus of shark from the Middle Triassic of Monte San Giorgio, Switzerland. Palaeontology 25:399–412.

Ritchie, A. 2005. *Cowralepis*, a new genus of phyllolepid fish (Pisces, Placodermi) from the Late Middle Devonian of New South Wales, Australia. Proceedings of the Linnean Society of New South Wales 126:215–259.

Schaeffer, B. 1981. The xenacanth shark neurocranium, with comments on elasmobranch monophyly.

Bulletin of the American Museum of Natural History 169:1–66.

Seidel, R., M. Blumer, P. Zaslansky, D. Knötel, D. R. Huber, J. C. Weaver, P. Fratzl, S. Omelon, L. Bertinetti, and M. N. Dean. 2017. Ultrastructural, material and crystallographic description of endophytic masses – A possible damage response in shark and ray tessellated calcified cartilage. Journal of Structural Biology 198:5–18.

Seidel, R., K. Lyons, M. Blumer, P. Zaslansky, P. Fratzl, J. C. Weaver, and M. N. Dean. 2016. Ultrastructural and developmental features of the tessellated endoskeleton of elasmobranchs (sharks and rays). Journal of Anatomy 229:681–702.

Soares, K. D. A. and M. R. De Carvalho. 2019. The catshark genus *Scyliorhinus* (Chondrichthyes: Carcharhiniformes: Scyliorhinidae): taxonomy, morphology, and distribution. Zootaxa 4601(1):1–147.

Solér-Gijon, R. & Hampe, O. 1998. Evidence of *Triodus* Jordan 1849 (Elasmobranchii: Xenacanthidae) in the Lower Permian of the Autun basin (Muse, France). *N. Jb. Geol. Paläont. Mh*. 1998, 335–348.

Stahl, B. J. 1999. Chondrichthyes III: Holocephali; pp. in H.-P. Schultze (ed.), Handbook of Paleoichthyology. Verlag Dr. Friedrich Pfeil, München, Germany.

Thomson, K. S. 1982. An early Triassic hybodont shark from northern Madagascar. Postilla 1–16.

Turner, S., Burrow, C. J. & Warren, A. 2005. *Gyracanthides hawkinsi* sp. nov. (Acanthodii, Gyracanthidae) from the Lower Carboniferous of Queensland, Australia, with a review of gyracanthid taxa. Palaeontology 48:963–1006.

Warren, A., Currie, B. P., Burrow, C. & Turner, S. 2000. A redescription and reinterpretation of *Gyracanthides murrayi* Woodward 1906 (Acanthodii, Gyracanthidae) from the Lower Carboniferous of the Mansfield Basin, Victoria, Australia. Journal of Vertebrate Paleontology 20:225–242.

Watson, D.M.S., 1937. II-The acanthodian fishes. Philosophical Transactions of the Royal Society of London. Series B, Biological Sciences 228(549):49–146.

Whitenack, L. B., D. C. Simkins, and P. J. Motta. 2011. Biology meets engineering: The structural mechanics of fossil and extant shark teeth. Journal of Morphology 272:169–179.

Wilga, C. D. 2002. A functional analysis of jaw suspension in elasmobranchs. Biological Journal of the Linnean Society 75(4):483–502.

Williams, M. E. 2001. Tooth retention in cladodont sharks: with a comparison between primitive grasping and swallowing, and modern cutting and gouging feeding mechanisms. Journal of Vertebrate Paleontology 21:214–226.

Woodward, A. S. and E. I. White. 1938. The dermal tubercles of the Upper Devonian shark, *Cladoselache*. Annals and Magazine of Natural History 11:367–368.

Young, G. C. 1982. Devonian sharks from southeastern Australia and Antarctica. Palaeontology, 25:817–843.

Yu, X. 1998. A new porolepiform-like fish, *Psarolepis romeri*, gen. et sp. nov. (Sarcopterygii, Osteichthyes) from the Lower Devonian of Yunnan, China. Journal of Vertebrate Paleontology 18:261–264.

Zangerl, R. 1981. Handbook of Paleoichthyology Volume 3A: Chondrichthyes I, Paleozoic Elasmobranchii (H.-P. Schultze (ed.)). Gustav Fischer Verlag, Stuttgart.

Zangerl, R., and G. R. Case. 1973. Iniopterygia: A new order of chondrichthyan fishes from the Pennsylvanian of North America. Fieldiana Geology Memoirs, Field Museum of Natural History, 67 pp.

Zhu, M. 2002. A primitive fish close to the common ancestor of tetrapods and lungfish. Nature 418:767–770.

Zhu, M., and H. P. Schultze. 1997. The oldest sarcopterygian fish. Lethaia 30:293–304.

Zhu, M., and H. P. Schultze. 2001. Interrelationships of basal osteichthyans; pp. 289–314 in P. E. Ahlberg (ed.), Major Events in Early Vertebrate Evolution. CRC Press.

Zhu, M., X. Yu., and P. Janvier, P. 1999. A primitive fossil fi sh sheds light on the origin of bony fishes. Nature 397:607–610.

Zhu, M., X. Yu, and P. E. Ahlberg. 2001. A primitive sarcopterygian fish with an eyestalk. Nature 410:81–84.

Zhu, M., W. Zhao, L. Jia, J. Lu, T. Qiao, and Q. Qu. 2009. The oldest articulated osteichthyan reveals mosaic gnathostome characters. Nature 458:469–474.

Zhu, M., X. Yu, P. E. Ahlberg, B.Choo, J. Lu, Q. Qiao, L. J. Zhao, H. Blom, and Y. Zhu. 2013. A Silurian placoderm with osteichthyan- like marginal jaw bones. Nature 52:188–193.

Zhu, M., P. E. Ahlberg, Z. Pan, Y. Zhu, T. Qiao, and W. Zhao. 2016. A new Silurian maxillate placoderm illuminates jaw evolution. Science 354:334–336.

Zidek, J. 1992. Late Pennsylvanian Chondrichthyes, Acanthodii, and deep-bodied Actinopterygii from the Kinney Quarry, Manzanita Moutains, New Mexico. In J. Zidek (ed.) Geology and paleontology of the Kinney Brick Quarry, Late Pennsylvanian, central New Mexico. Bulletin 138, New Mexico Bureau of Mines & Mineral Resources (Socorro: New Mexico Bureau of Mines & Mineral Resources), pp. 199-214.